Cell membranes and perivascular pathways:

a finite element tale of dimensional gaps

Marie E. Rognes

Department of Numerical Analysis and Scientific Computing
Simula Research Laboratory, Oslo, Norway

K. G. Jebsen Centre for Brain Fluid Research

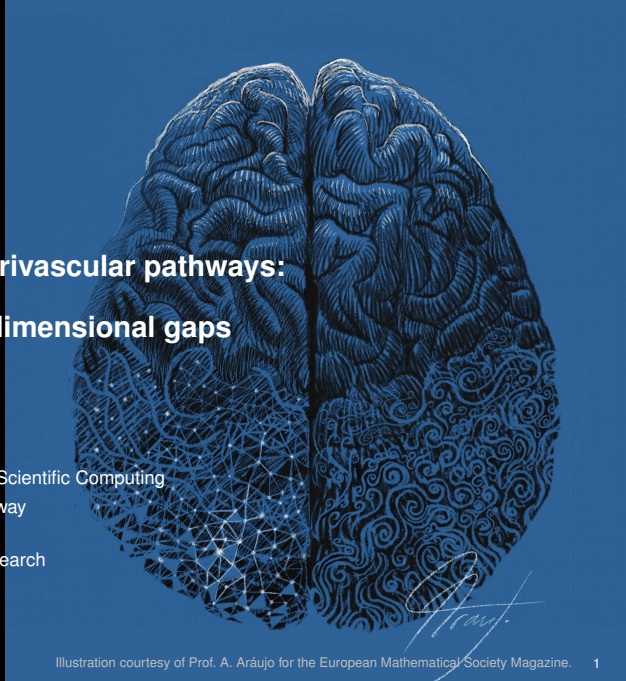

Illustration courtesy of Prof. A. Aráujo for the European Mathematical Society Magazine.

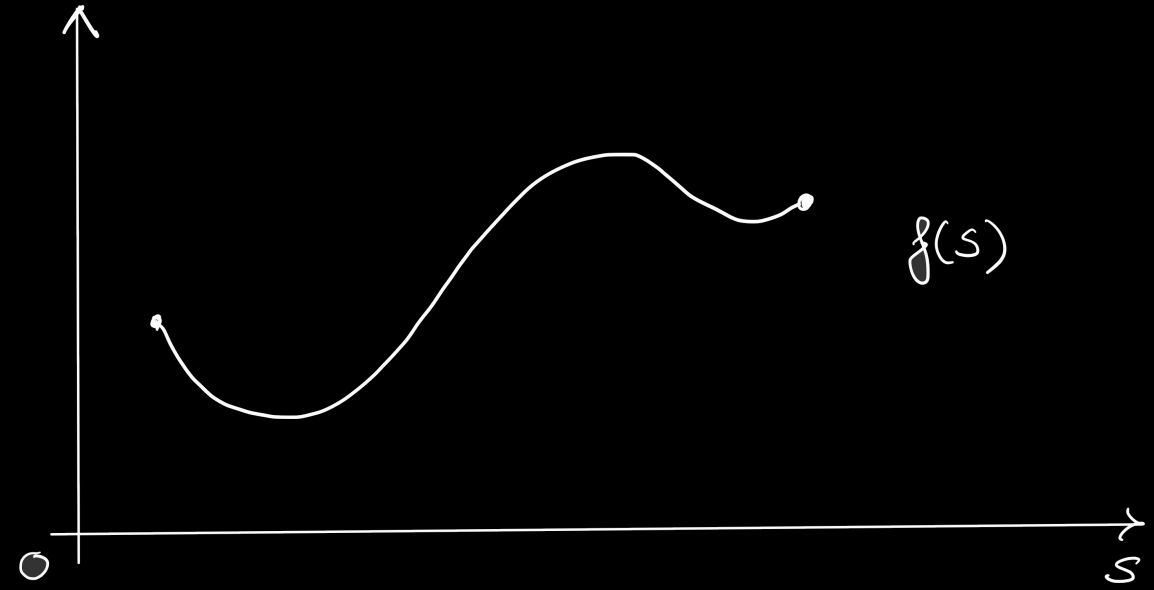
f(s)
0
s

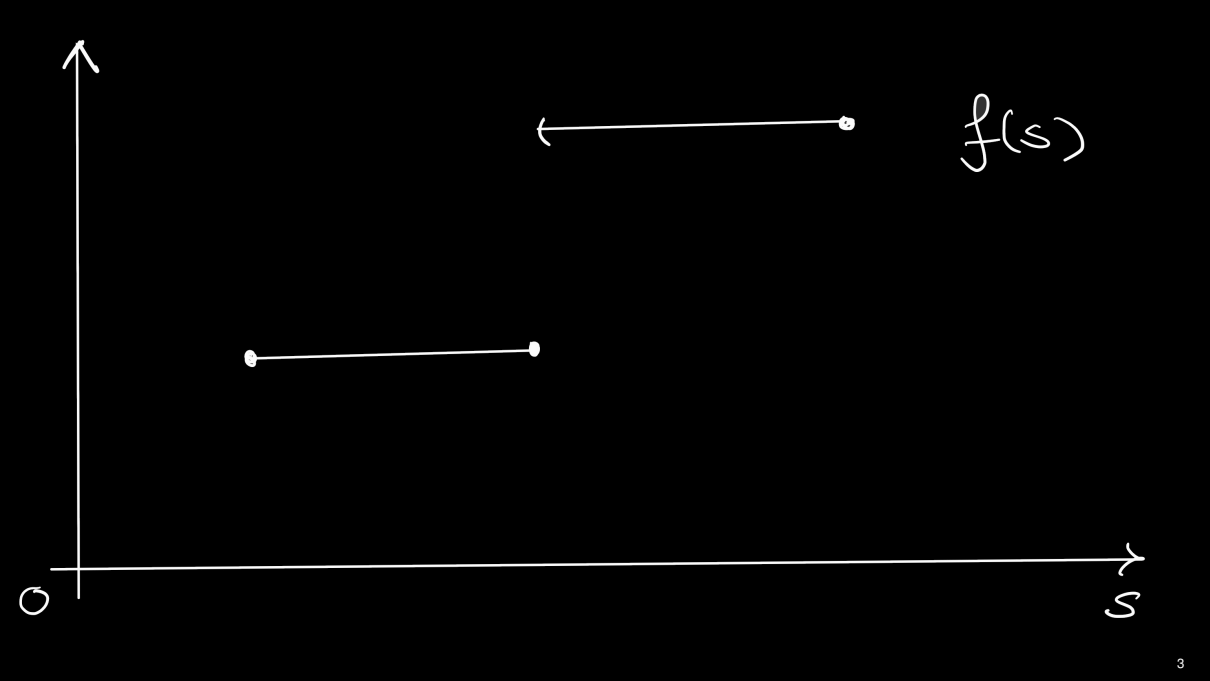
f(s)
0
s

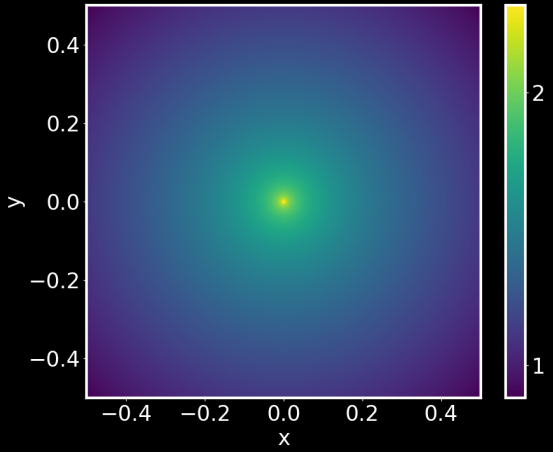

$$u(x,y) = (-\ln(x^2+y^2))^{\frac{1}{3}}$$

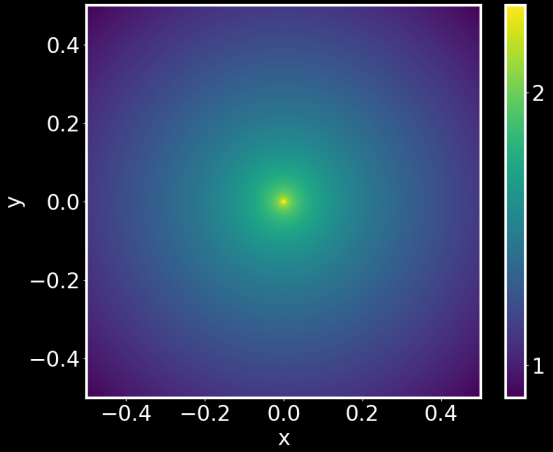

For $\Omega \subset \mathbb{R}^d$ $(d > 1)$, $u \in H^1(\Omega)$ need not be continuous; e.g.

$$u(x, y) = (-\ln(x^2 + y^2))^{\frac{1}{3}} \in H^1(\Omega)$$

Continuity and the trace theorem in Laplace boundary value problems

Define $u \in H^1_g(\Omega) \equiv W^{1,2}_g(\Omega)$ such that

$$\int_\Omega \nabla u \cdot \nabla v \, \mathrm{d}x = 0 \quad \forall\, v \in H^1_0(\Omega)$$

where $H^1_g = \{u \in L^2 \mid \nabla u \in L^2 \mid \operatorname{tr} u = g\}$

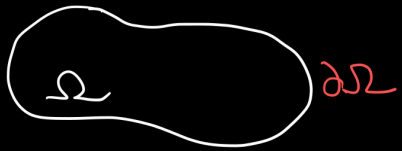

Continuity and the trace theorem in Laplace boundary value problems

Define $u \in H^1_g(\Omega) \equiv W^{1,2}_g(\Omega)$ such that

$$\int_\Omega \nabla u \cdot \nabla v \, \mathrm{d}x = 0 \quad \forall\, v \in H^1_0(\Omega)$$

where $H^1_g = \{u \in L^2 \mid \nabla u \in L^2 \mid \operatorname{tr} u = g\}$

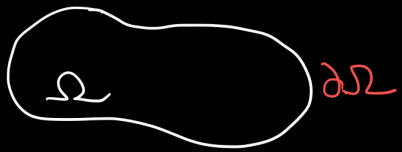

In what sense is u solving

$$\begin{aligned} -\nabla\cdot\nabla u &= 0 \quad && \text{in } \Omega, \\ u &= g \quad && \text{on } \partial\Omega, \end{aligned}$$

in terms of continuity?

Continuity and the trace theorem in Laplace boundary value problems

Define $u \in H^1_g(\Omega) \equiv W^{1,2}_g(\Omega)$ such that

$$\int_\Omega \nabla u \cdot \nabla v \, \mathrm{d}x = 0 \quad \forall\, v \in H^1_0(\Omega)$$

where $H^1_g = \{u \in L^2 \mid \nabla u \in L^2 \mid \operatorname{tr} u = g\}$

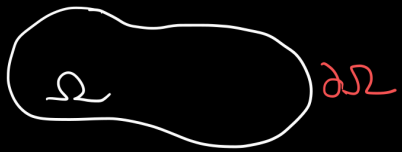

In what sense is u solving

$$\begin{aligned} -\nabla\cdot\nabla u &= 0 \quad && \text{in } \Omega, \\ u &= g \quad && \text{on } \partial\Omega, \end{aligned}$$

in terms of continuity?

Theorem (Trace theorem)

Assume that Ω is bounded and Lipschitz. There exists a linear operator $\operatorname{tr} : W^{1,p}(\Omega) \to L^p(\partial\Omega)$ such that for $1 \leqslant p < \infty$

$$\begin{aligned} \operatorname{tr} u &= u|_{\partial\Omega}, && \forall\, u \in W^{1,p} \cap C(\bar{\Omega}), \\ \|\operatorname{tr} u\|_{L^p(\partial\Omega)} &\lesssim \|u\|_{W^{1,p}(\Omega)} && \forall\, u \in W^{1,p}(\Omega). \end{aligned}$$

Codimension 1: brain membranes and the ionic landscape

From Sobolev inequalities to computational life science multiphysics (and back again)

Laughlin et al. [2023]

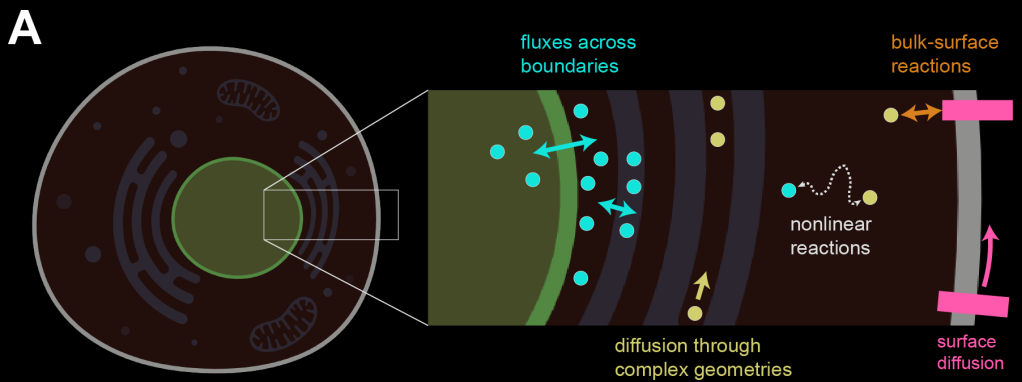

Theorem (Trace theorem ($H^1(\Omega) = W^{1,2}(\Omega)$))

Assume that Ω is bounded and Lipschitz. There exists a linear operator $\mathrm{tr} : H^1(\Omega) \to H^{\frac{1}{2}}(\partial\Omega) \subset L^2(\partial\Omega)$ *such that*

$$\mathrm{tr}\, u = u|_{\partial\Omega}, \quad \forall\, u \in H^1 \cap C(\bar{\Omega}), \qquad \|\mathrm{tr}\, u\|_{L^2(\partial\Omega)} \lesssim \|u\|_{H^1(\Omega)} \quad \forall\, u \in H^1(\Omega).$$

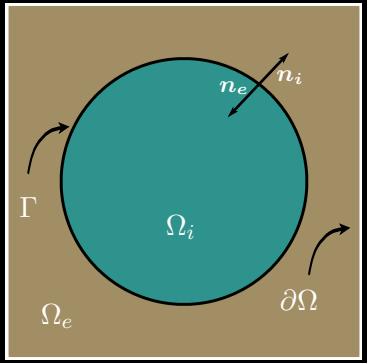

Ben Belgacem et al. [2015], (Illustration courtesy of Nanna Berre)

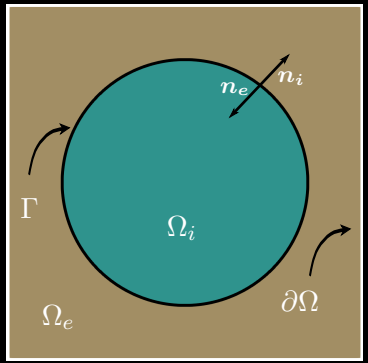

Let $u_i : \Omega_i \to \mathbb{R}$ and $u_e : \Omega_e \to \mathbb{R}$.

Diffusion separated by the interface Γ

$$-\Delta u_i = 0 \qquad \text{in } \Omega_i$$
$$-\Delta u_e = 0 \qquad \text{in } \Omega_e$$

Ben Belgacem et al. [2015], (Illustration courtesy of Nanna Berre)

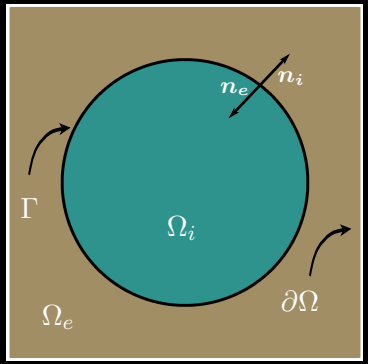

Let $u_i : \Omega_i \to \mathbb{R}$ and $u_e : \Omega_e \to \mathbb{R}$.

Diffusion separated by the interface Γ

$$-\Delta u_i = 0 \qquad \text{in } \Omega_i$$
$$-\Delta u_e = 0 \qquad \text{in } \Omega_e$$

Interface conditions that allow for jumps in u

$$-\nabla u_i \cdot n_i = \nabla u_e \cdot n_e \qquad \text{on } \Gamma$$
$$[\![u]\!] \equiv u_i - u_e = g \qquad \text{on } \Gamma$$

Ben Belgacem et al. [2015], (Illustration courtesy of Nanna Berre)

Modelling (excitable) biological cells via geometrical cells: the dynamics of extracellular, membrane and intracellular potentials

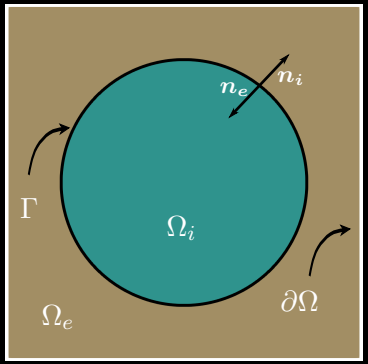

Intracellular and extracellular potentials u_i, u_e

$$-\Delta u_i = 0 \qquad \text{in } \Omega_i$$
$$-\Delta u_e = 0 \qquad \text{in } \Omega_e$$

Stinstra et al. [2010], Agudelo-Toro and Neef [2013], Tveito et al. [2017, 2021], ...

Modelling (excitable) biological cells via geometrical cells: the dynamics of extracellular, membrane and intracellular potentials

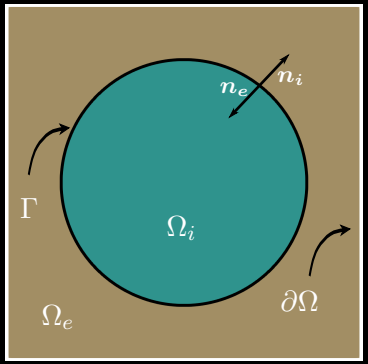

Intracellular and extracellular potentials u_i, u_e

$$-\Delta u_i = 0 \qquad \text{in } \Omega_i$$
$$-\Delta u_e = 0 \qquad \text{in } \Omega_e$$

Membrane potential v defined over Γ:

$$v = [\![u]\!] = u_i - u_e$$

Stinstra et al. [2010], Agudelo-Toro and Neef [2013], Tveito et al. [2017, 2021], ...

Modelling (excitable) biological cells via geometrical cells: the dynamics of extracellular, membrane and intracellular potentials

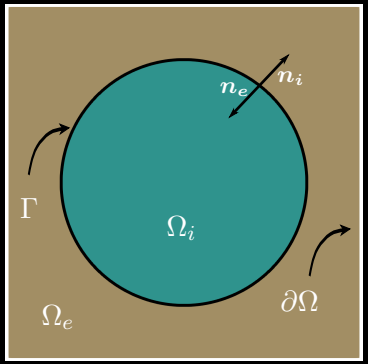

Intracellular and extracellular potentials u_i, u_e

$$-\Delta u_i = 0 \qquad \text{in } \Omega_i$$
$$-\Delta u_e = 0 \qquad \text{in } \Omega_e$$

Membrane potential v defined over Γ:

$$v = [\![u]\!] = u_i - u_e$$

Conservation of current I_m

$$-\nabla u_i \cdot n_i = \nabla u_e \cdot n_e \equiv I_m \qquad \text{on } \Gamma$$

Stinstra et al. [2010], Agudelo-Toro and Neef [2013], Tveito et al. [2017, 2021], ...

Modelling (excitable) biological cells via geometrical cells: the dynamics of extracellular, membrane and intracellular potentials

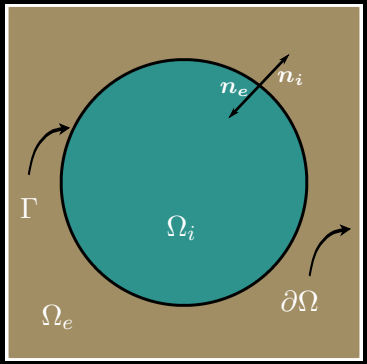

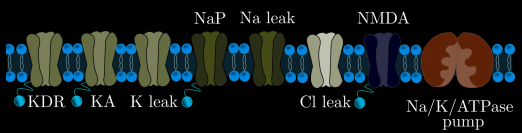

Molecular channels and pumps regulate interface dynamics

Intracellular and extracellular potentials u_i, u_e

$$-\Delta u_i = 0 \qquad \text{in } \Omega_i$$
$$-\Delta u_e = 0 \qquad \text{in } \Omega_e$$

Membrane potential v defined over Γ:

$$v = [\![u]\!] = u_i - u_e$$

Conservation of current I_m

$$-\nabla u_i \cdot n_i = \nabla u_e \cdot n_e \equiv I_m \qquad \text{on } \Gamma$$

... across an active interface – for $t > 0$

$$\partial_t [\![u]\!] = I_m - f(u, \dots) \qquad \text{on } \Gamma$$

Stinstra et al. [2010], Agudelo-Toro and Neef [2013], Tveito et al. [2017, 2021], ...

The geometry representation is key to study the role of morphology and heterogeneities

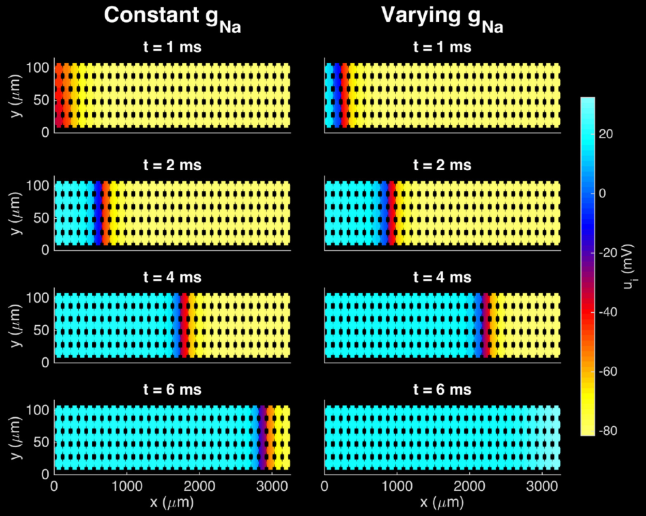

Tveito et al. [2017] (Simulations courtesy of Karoline Jæger)

How to solve EMI-type equations?

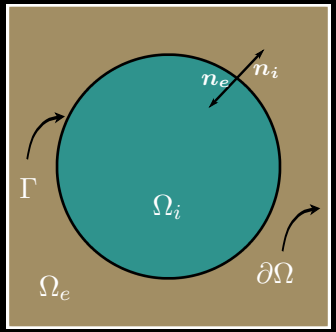

EMI equations for $r \in \{i, e\}$

$$-\Delta u_r = 0 \qquad \text{in } \Omega_r$$

Interface condition (time step τ)

$$\tau^{-1}[\![u]\!] = I_m - f(\cdots), \quad I_m = \nabla u_e \cdot n_e$$

How to solve EMI-type equations?

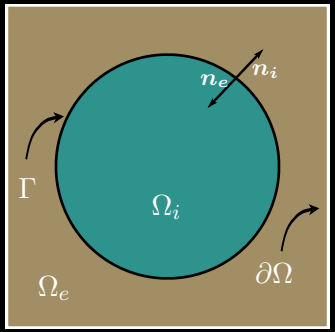

Recall integration by parts

$$(-\Delta u, v)_\Omega = (\nabla u, \nabla v)_\Omega - (\nabla u \cdot n, v)_{\partial\Omega}$$

where $(u, v)_D = \int_D uv$.

EMI equations for $r \in \{i, e\}$

$$-\Delta u_r = 0 \qquad \text{in } \Omega_r$$

Interface condition (time step τ)

$$\tau^{-1}[\![u]\!] = I_m - f(\cdots), \quad I_m = \nabla u_e \cdot n_e$$

How to solve EMI-type equations?

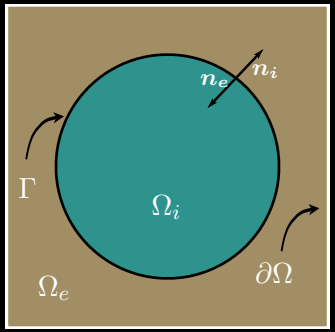

Recall integration by parts

$$(-\Delta u, v)_\Omega = (\nabla u, \nabla v)_\Omega - (\nabla u \cdot n, v)_{\partial\Omega}$$

where $(u, v)_D = \int_D uv$.

EMI equations for $r \in \{i, e\}$

$$-\Delta u_r = 0 \qquad \text{in } \Omega_r$$

Interface condition (time step τ)

$$\tau^{-1}[\![u]\!] = I_m - f(\cdots), \quad I_m = \nabla u_e \cdot n_e$$

Eliminate $I_m \rightarrow$
single-dimensional formulation

Find $u_i \in H^1(\Omega_i)$, $u_e \in H^1(\Omega_e)$ such that

$$(\nabla u_e, \nabla v_e)_{\Omega_e} - \tau^{-1}([\![u]\!], v_e)_\Gamma = (f, v_e)_\Gamma$$
$$(\nabla u_i, \nabla v_i)_{\Omega_i} + \tau^{-1}([\![u]\!], v_i)_\Gamma = -(f, v_i)_\Gamma$$

for all $v_i \in H^1(\Omega_i)$, $v_e \in H^1(\Omega_e)$

Kuchta et al. [2021], Tveito et al. [2021]

Single-dimensional formulations of EMI equations fail for small time steps ($\tau \to 0$)

How to solve EMI-type equations?

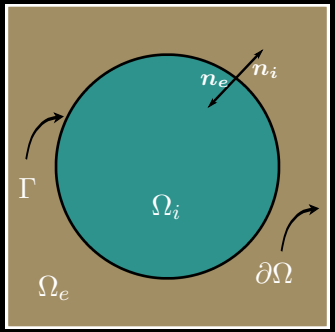

Recall integration by parts

$$(-\Delta u, v)_\Omega = (\nabla u, \nabla v)_\Omega - (\nabla u \cdot n, v)_{\partial\Omega}$$

where $(u, v)_D = \int_D uv.$

EMI equations for $r \in \{i, e\}$

$$-\Delta u_r = 0 \qquad \text{in } \Omega_r$$

Interface condition (time step τ)

$$\tau^{-1}[\![u]\!] = I_m - f(\cdots), \quad I_m = \nabla u_e \cdot n_e$$

Eliminate $I_m \to$
single-dimensional formulation

Find $u_i \in H^1(\Omega_i)$, $u_e \in H^1(\Omega_e)$ such that

$$(\nabla u_e, \nabla v_e)_{\Omega_e} - \tau^{-1}([\![u]\!], v_e)_\Gamma = (f, v_e)_\Gamma$$
$$(\nabla u_i, \nabla v_i)_{\Omega_i} + \tau^{-1}([\![u]\!], v_i)_\Gamma = -(f, v_i)_\Gamma$$

for all $v_i \in H^1(\Omega_i)$, $v_e \in H^1(\Omega_e)$

Kuchta et al. [2021], Tveito et al. [2021]

How to solve EMI-type equations?

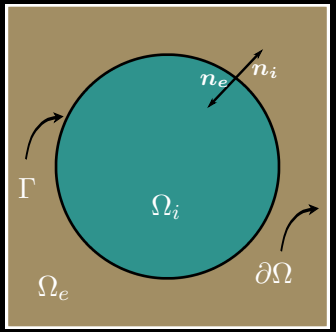

EMI equations for $r \in \{i, e\}$

$$-\Delta u_r = 0 \qquad \text{in } \Omega_r$$

Interface condition (time step τ)

$$\tau^{-1}[\![u]\!] = I_m - f(\cdots), \quad I_m = \nabla u_e \cdot n_e$$

How to solve EMI-type equations?

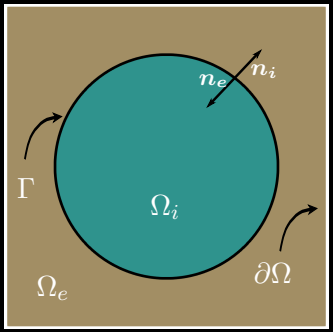

EMI equations for $r \in \{i, e\}$

$$-\Delta u_r = 0 \qquad \text{in } \Omega_r$$

Interface condition (time step τ)

$$\tau^{-1}[\![u]\!] = I_m - f(\cdots), \quad I_m = \nabla u_e \cdot n_e$$

Keep $I_m \rightarrow$ multi-dimensional formulation

Wohlmuth [2000], Tveito et al. [2017], Kuchta et al. [2021]

How to solve EMI-type equations?

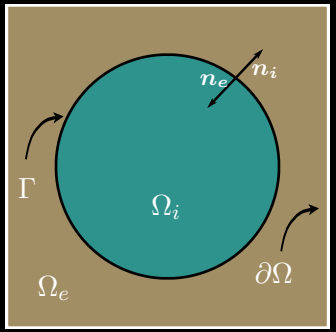

EMI equations for $r \in \{i, e\}$

$$-\Delta u_r = 0 \qquad \text{in } \Omega_r$$

Interface condition (time step τ)

$$\tau^{-1}[\![u]\!] = I_m - f(\cdots), \quad I_m = \nabla u_e \cdot n_e$$

Keep $I_m \rightarrow$ multi-dimensional formulation

Find $u_i \in H^1(\Omega_i)$, $u_e \in H^1(\Omega_e)$, $I_m \in X(\Gamma)$

$$(\nabla u_e, \nabla v_e)_{\Omega_e} - (I_m, v_e)_\Gamma = 0$$
$$(\nabla u_i, \nabla v_i)_{\Omega_i} + (I_m, v_i)_\Gamma = 0$$

for all $v_i \in H^1(\Omega_i)$, $v_e \in H^1(\Omega_e)$,

Wohlmuth [2000], Tveito et al. [2017], Kuchta et al. [2021]

How to solve EMI-type equations?

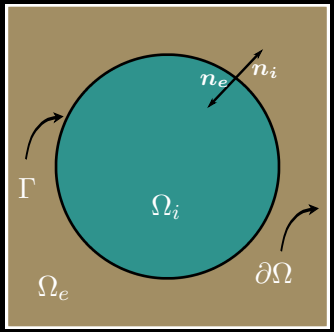

EMI equations for $r \in \{i, e\}$

$$-\Delta u_r = 0 \qquad \text{in } \Omega_r$$

Interface condition (time step τ)

$$\tau^{-1}[\![u]\!] = I_m - f(\cdots), \quad I_m = \nabla u_e \cdot n_e$$

Keep $I_m \rightarrow$ multi-dimensional formulation

Find $u_i \in H^1(\Omega_i)$, $u_e \in H^1(\Omega_e)$, $I_m \in X(\Gamma)$

$$(\nabla u_e, \nabla v_e)_{\Omega_e} - (I_m, v_e)_\Gamma = 0$$
$$(\nabla u_i, \nabla v_i)_{\Omega_i} + (I_m, v_i)_\Gamma = 0$$
$$([\![u]\!], \iota)_\Gamma - \tau(I_m, \iota)_\Gamma = (f, \iota)_\Gamma$$

for all $v_i \in H^1(\Omega_i)$, $v_e \in H^1(\Omega_e)$, $\iota \in X^*(\Gamma)$

Wohlmuth [2000], Tveito et al. [2017], Kuchta et al. [2021]

Multi-dim. EMI formulations are well-posed in the limit $\tau \to 0$, but require compatibility

How to solve EMI-type equations?

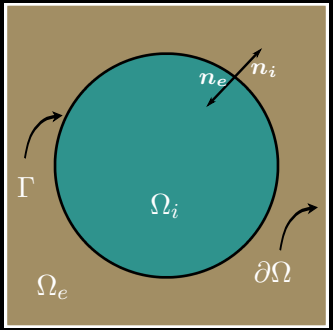

$X(\Gamma) = H^{\frac{1}{2}}(\Gamma), X^*(\Gamma) = H^{-\frac{1}{2}}(\Gamma)$

EMI equations for $r \in \{i, e\}$

$$-\Delta u_r = 0 \qquad \text{in } \Omega_r$$

Interface condition (time step τ)

$$\tau^{-1}[\![u]\!] = I_m - f(\cdots), \quad I_m = \nabla u_e \cdot n_e$$

Keep $I_m \to$ multi-dimensional formulation

Find $u_i \in H^1(\Omega_i)$, $u_e \in H^1(\Omega_e)$, $I_m \in X(\Gamma)$

$$(\nabla u_e, \nabla v_e)_{\Omega_e} - (I_m, v_e)_\Gamma = 0$$
$$(\nabla u_i, \nabla v_i)_{\Omega_i} + (I_m, v_i)_\Gamma = 0$$
$$([\![u]\!], \iota)_\Gamma - \tau(I_m, \iota)_\Gamma = (f, \iota)_\Gamma$$

for all $v_i \in H^1(\Omega_i)$, $v_e \in H^1(\Omega_e)$, $\iota \in X^*(\Gamma)$

Wohlmuth [2000], Tveito et al. [2017], Kuchta et al. [2021]

Multi-dim. EMI formulations are well-posed in the limit $\tau \to 0$, but require compatibility

How to solve EMI-type equations?

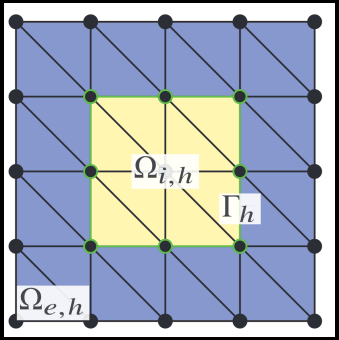

$$X(\Gamma) = H^{\frac{1}{2}}(\Gamma),\ X^*(\Gamma) = H^{-\frac{1}{2}}(\Gamma)$$

$$X_h \approx \mathrm{tr}(U_h)$$

EMI equations for $r \in \{i, e\}$

$$-\Delta u_r = 0 \qquad \text{in } \Omega_r$$

Interface condition (time step τ)

$$\tau^{-1}[\![u]\!] = I_m - f(\cdots), \quad I_m = \nabla u_e \cdot n_e$$

Keep $I_m \to$ multi-dimensional formulation

Find $u_i \in H^1(\Omega_i)$, $u_e \in H^1(\Omega_e)$, $I_m \in X(\Gamma)$

$$(\nabla u_e, \nabla v_e)_{\Omega_e} - (I_m, v_e)_\Gamma = 0$$
$$(\nabla u_i, \nabla v_i)_{\Omega_i} + (I_m, v_i)_\Gamma = 0$$
$$([\![u]\!], \iota)_\Gamma - \tau(I_m, \iota)_\Gamma = (f, \iota)_\Gamma$$

for all $v_i \in H^1(\Omega_i)$, $v_e \in H^1(\Omega_e)$, $\iota \in X^*(\Gamma)$

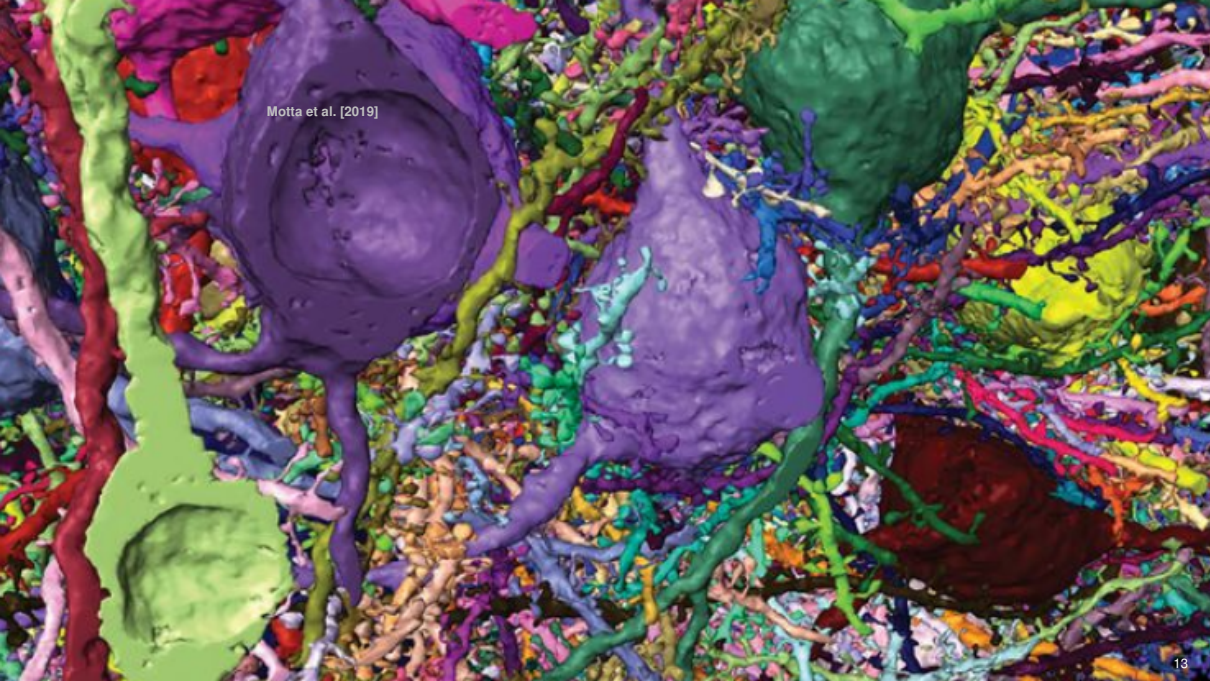
Motta et al. [2019]

Simulating an ionic landscape spanning neuronal, astrocytic and extracellular spaces

Calì et al. [2019], Abdellah et al. [2022], Benedusi et al. [2024]

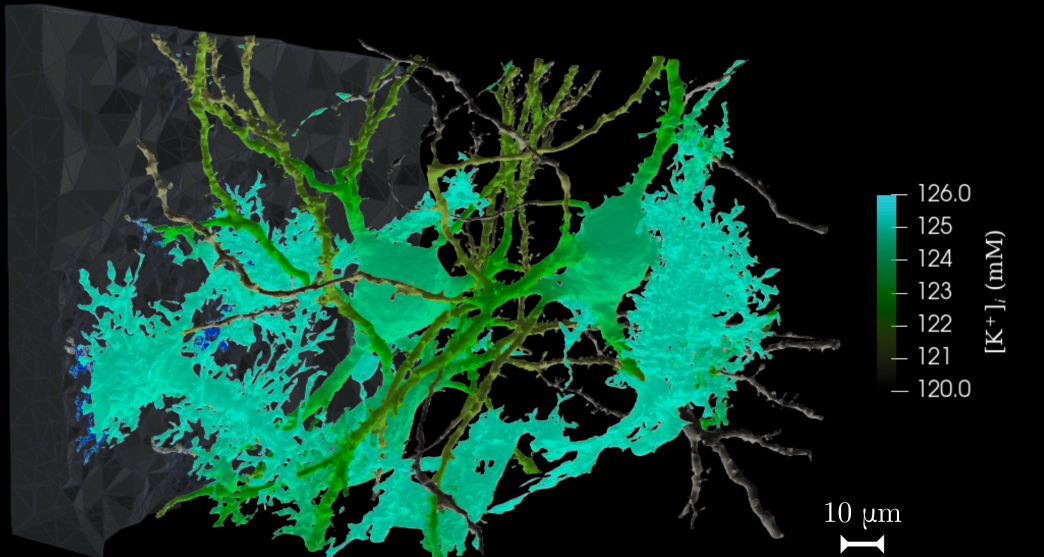

Electrodiffusion of $\{\mathrm{Na}^+, \mathrm{K}^+, \mathrm{Cl}^-\}$ in neurons, astrocytes and ECS, 100 million degrees of freedom.

Codimension 2: perivascular pathways and the brain’s waterscape

The dim-2 gap problem: when are traces with higher dimensional gaps well-defined?

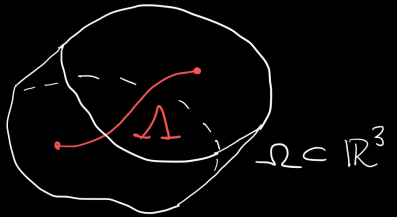

Consider a submanifold $\Lambda \subset \Omega$ of dimension $d-2$.

When is $u|_\Lambda$ well-defined and in what sense?

The dim-2 gap problem: when are traces with higher dimensional gaps well-defined?

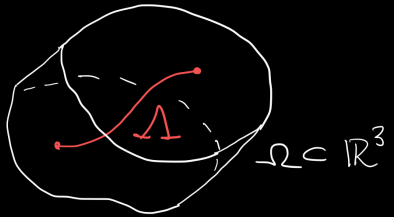

Consider a submanifold $\Lambda \subset \Omega$ of dimension $d-2$.

When is $u|_\Lambda$ well-defined and in what sense?

Theorem (Sobolev embedding theorem)
If $\Omega \subset \mathbb{R}^d$ is Lipschitz, then for $p \geq \frac{d}{2}$,

$$W^{2,p}(\Omega) \subseteq C(\bar{\Omega}).$$

Theorem (Morrey's inequality)
If $\Omega \subset \mathbb{R}^d$ is Lipschitz, then for $p > d$,

$$W^{1,p}(\Omega) \subseteq C(\Omega).$$

The dim-2 gap problem: when are traces with higher dimensional gaps well-defined?

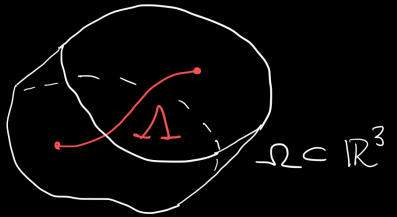

Consider a submanifold $\Lambda \subset \Omega$ of dimension $d-2$.

When is $u|_\Lambda$ well-defined and in what sense?

Not covering $u \in W^{1,2}(\Omega) \equiv H^1(\Omega)$ $(d \geqslant 2)$!

Theorem (Sobolev embedding theorem)
If $\Omega \subset \mathbb{R}^d$ is Lipschitz, then for $p \geq \frac{d}{2}$,

$$W^{2,p}(\Omega) \subseteq C(\bar{\Omega}).$$

Theorem (Morrey's inequality)
If $\Omega \subset \mathbb{R}^d$ is Lipschitz, then for $p > d$,

$$W^{1,p}(\Omega) \subseteq C(\Omega).$$

Systems of elliptic equations coupled between $d \times (d-2)$D domains

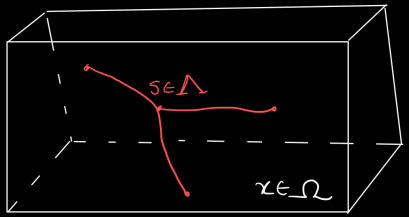

Example: tissue perfusion

Consider steady perfusion in a biological tissue represented by Ω and an embedded network of topologically one-dimensional blood vessels Λ.

Define spatial coordinates: $x \in \Omega \subset \mathbb{R}^d$ and $s \in \Lambda \subset \mathbb{R}$.

Find $u : \Omega \to \mathbb{R}$ and $\hat{u} : \Lambda \to \mathbb{R}$ such that

$$
\begin{aligned}
-\nabla \cdot (k \nabla u) - f(u, \hat{u}) &= 0 \quad \text{in } \Omega, \\
-\partial_s (\hat{k} \partial_s \hat{u}) + \hat{f}(u, \hat{u}) &= 0 \quad \text{in } \Lambda.
\end{aligned}
$$

Here, k and $\hat{k}$ are the respective hydraulic conductivities, and f and $\hat{f}$ represent the flux into Ω from Λ and into Λ from Ω, respectively.

$$
\hat{f}(u, \hat{u}) = \beta(\hat{u} - \bar{u}), \qquad \bar{u} = \|\partial C\|^{-1} \int_{\partial C} u \, \mathrm{d}\theta,
$$

$$
f(u, \hat{u}) = \hat{f}(u, \hat{u}) \delta_\Lambda.
$$

[D'Angelo and Quarteroni (2008)]

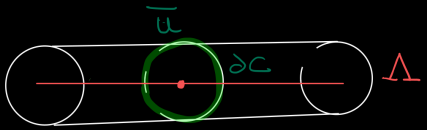

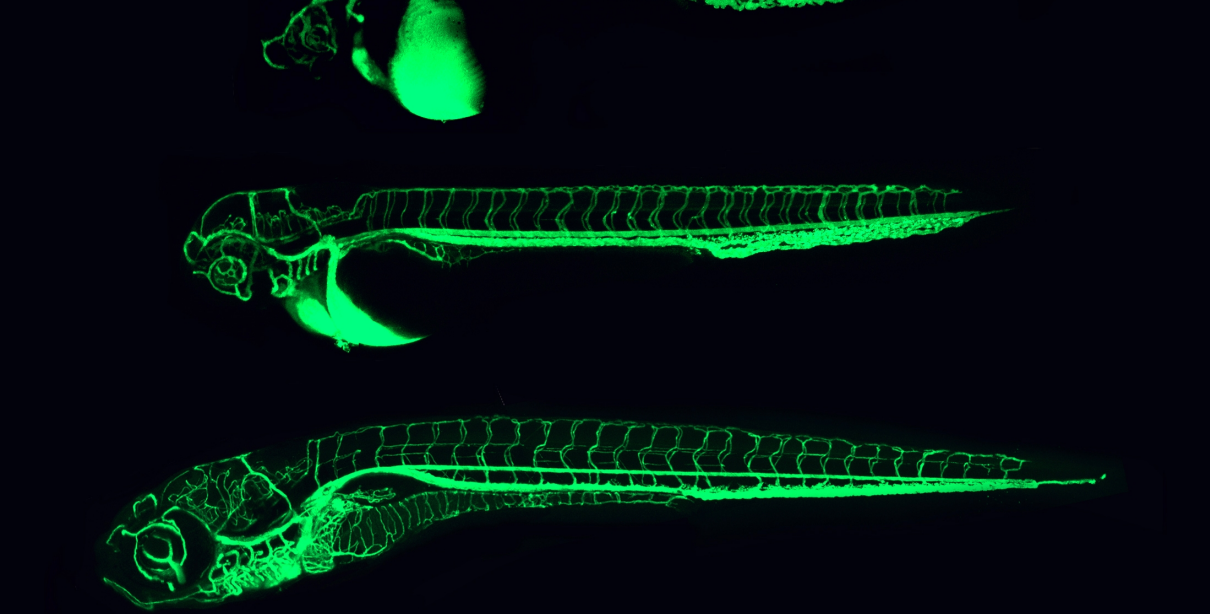

[Zebrafish vasculature, Eunice Kennedy Shriver National Institute of Child Health and Human Development]

[Lymphatic vessels, William Cruikshank, Wellcome Library, London]

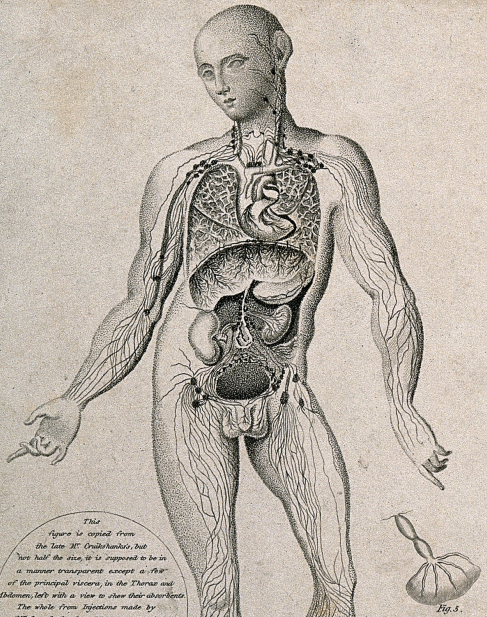

This figure is copied from the late Mr. Cruikshank's, but was half the size, it is supposed to be in a manner evanparent except a few of the principal viscera, in the Thorax and Abdomen, left with a view to shew their absorbents. The whole from Specalms made by

Fig. 5.

Mr. Cruikshanks 2d. Plate on the Absorbents, or his Work.

Fig. 1.

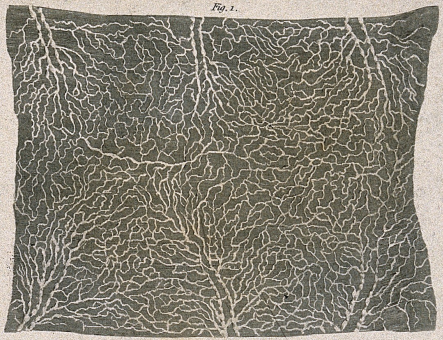

Fig. 2.

Fig. 3.

Fig. 4.

Dr. Baillie on the absorbent Vessels 1st & 2d Lectures, Windmill Street.

The Mark explained over leaf to in Pl. IV.

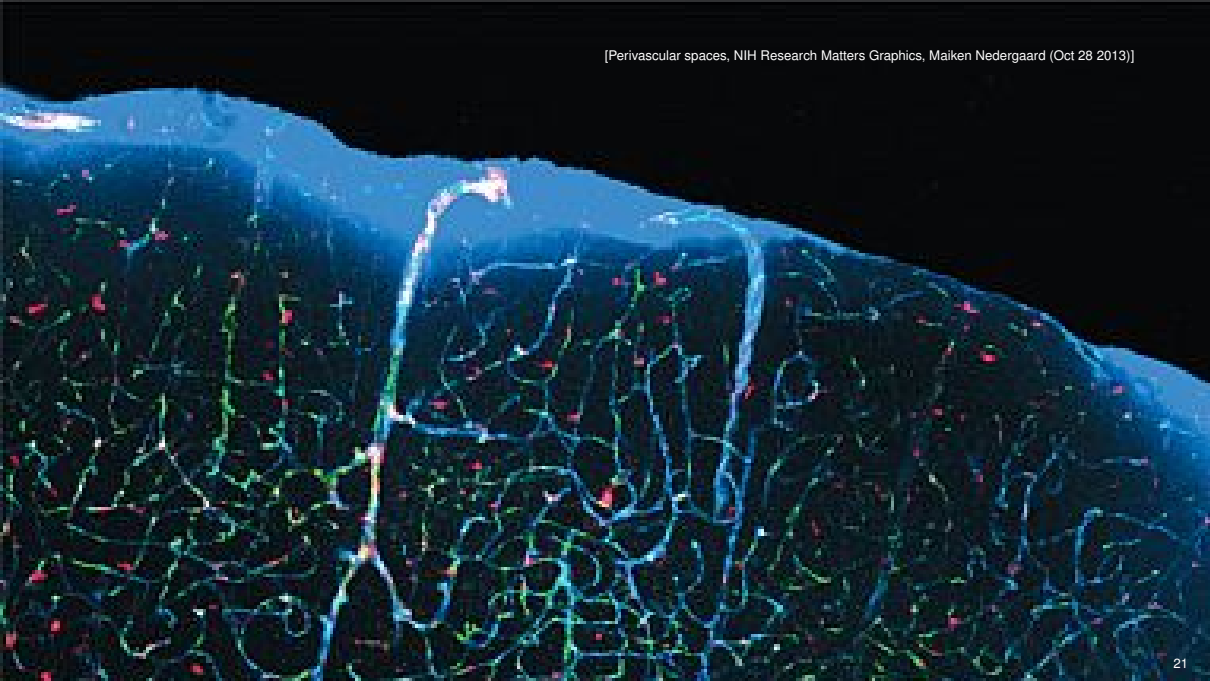

[Perivascular spaces, NIH Research Matters Graphics, Maiken Nedergaard (Oct 28 2013)]

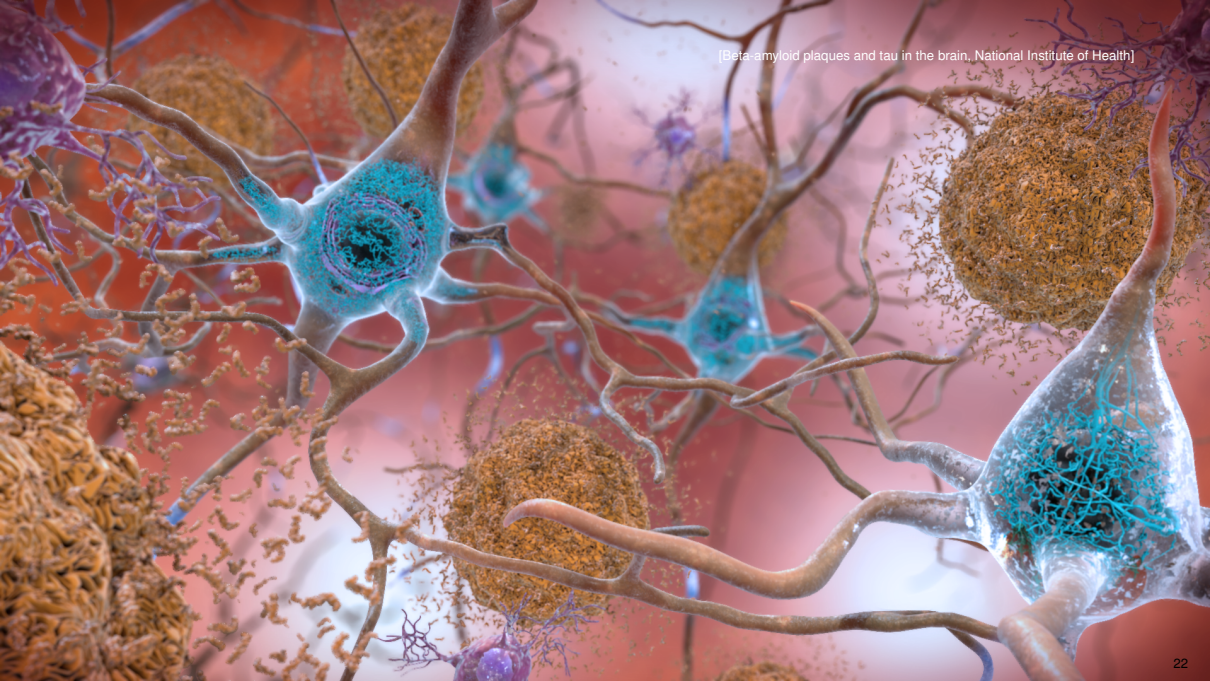

[Beta-amyloid plaques and tau in the brain, National Institute of Health]

Molecular transport via perivascular pathways underpins human brain clearance

His [1865], Flexner [1933], Rennels et al. [1985], Ichimura et al. [1991], Hadaczek et al. [2006], Iliff et al. [2012], Mestre et al. [2018] (Movie S2)

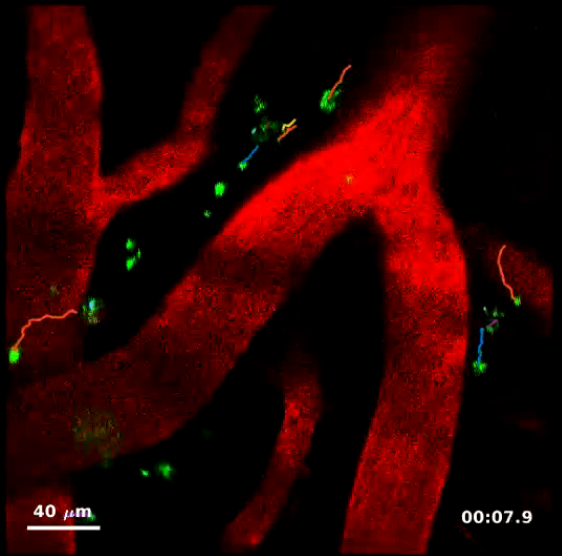

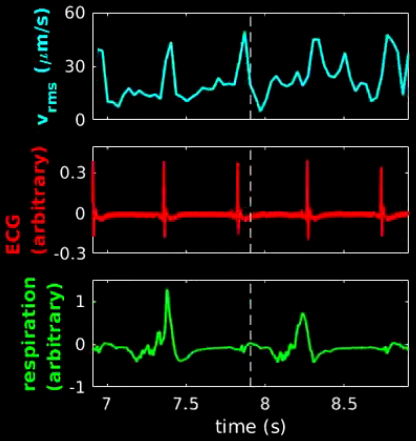

Pulsatile perivascular flow and transport patterns induced by long waves of wall motion

Daversin-Catty et al. [2020]

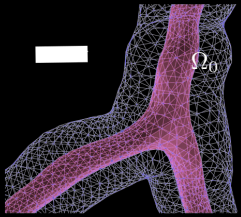

Scale bar: 50μm.

Sangalli et al. [2014] (Aneurisk data set), San Martín et al. [2009] (ALE), Asgari et al. [2016], Thomas [2019], Martinac and Bilston [2020]

Pulsatile perivascular flow and transport patterns induced by long waves of wall motion

Daversin-Catty et al. [2020]

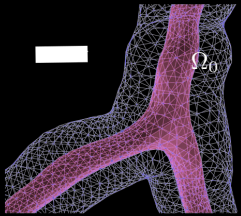

Scale bar: 50μm.

Incompressible Stokes

Find the velocity v and pressure p s.t.

$$\begin{aligned} \partial_t v - \nu \nabla^2 v + \nabla p &= 0 \quad \text{in } \Omega(t) \\ \nabla \cdot v &= 0 \quad \text{in } \Omega(t) \end{aligned}$$

where $\Omega(t) \overset{d}{\leftarrow\!\shortmid} \Omega_0$ for $t > 0$.

Domain motion

The vascular (inner) wall Γ_w expands and contracts by a travelling pulse wave ($f \approx 1 - 10$Hz, $c \approx 1$m/s)

$$v|_{\Gamma_w} = \partial_t d|_{\Gamma_w}.$$

Discretization

Arbitrary Eulerian-Lagrangian (ALE) finite element (Taylor–Hood) formulation (optimal convergence)

Sangalli et al. [2014] (Aneurisk data set), San Martín et al. [2009] (ALE), Asgari et al. [2016], Thomas [2019], Martinac and Bilston [2020]

Pulsatile perivascular flow and transport patterns induced by long waves of wall motion

Daversin-Catty et al. [2020]

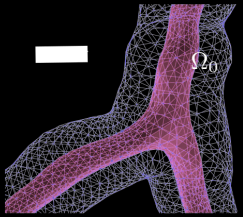

Scale bar: 50μm.

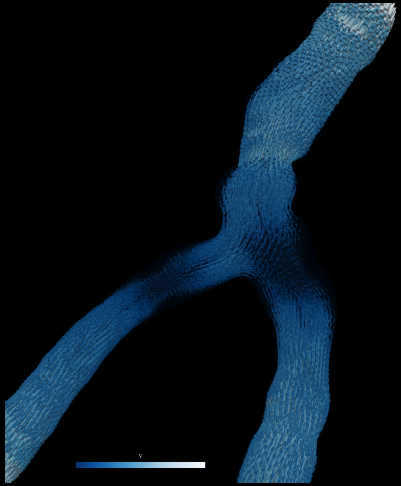

Incompressible Stokes

Find the velocity v and pressure p s.t.

$$\begin{aligned} \partial_t v - \nu \nabla^2 v + \nabla p = 0 \quad & \text{in } \Omega(t) \\ \nabla \cdot v = 0 \quad & \text{in } \Omega(t) \end{aligned}$$

where $\Omega(t) \overset{d}{\hookleftarrow} \Omega_0$ for $t > 0$.

Domain motion

The vascular (inner) wall Γ_w expands and contracts by a travelling pulse wave ($f \approx 1 - 10$Hz, $c \approx 1$m/s)

$$v|_{\Gamma_w} = \partial_t d|_{\Gamma_w}.$$

Discretization

Arbitrary Eulerian-Lagrangian (ALE) finite element (Taylor–Hood) formulation (optimal convergence)

Sangalli et al. [2014] (Aneurisk data set), San Martín et al. [2009] (ALE), Asgari et al. [2016], Thomas [2019], Martinac and Bilston [2020]

Pulsatile perivascular flow and transport patterns induced by long waves of wall motion

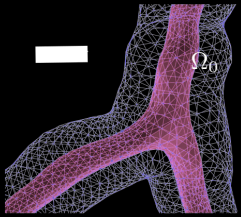

Scale bar: 50μm.

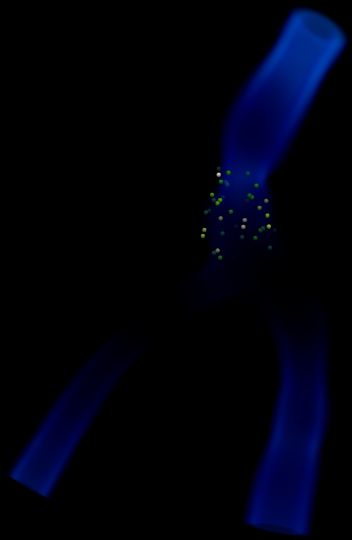

Daversin-Catty et al. [2020]

Incompressible Stokes

Find the velocity v and pressure p s.t.

$$\begin{aligned} \partial_t v - \nu \nabla^2 v + \nabla p &= 0 \quad \text{in } \Omega(t) \\ \nabla \cdot v &= 0 \quad \text{in } \Omega(t) \end{aligned}$$

where $\Omega(t) \overset{d}{\leftarrow} \Omega_0$ for $t > 0$.

Domain motion

The vascular (inner) wall Γ_w expands and contracts by a travelling pulse wave ($f \approx 1 - 10$Hz, $c \approx 1$m/s)

$$v|_{\Gamma_w} = \partial_t d|_{\Gamma_w}.$$

Discretization

Arbitrary Eulerian-Lagrangian (ALE) finite element (Taylor–Hood) formulation (optimal convergence)

Geometrically-reduced models accurately represent pulsatile flow in perivascular networks

Hodneland et al. [2019] **(Vascular data),** Olufsen [1999], Formaggia et al. [2003] Daversin-Catty et al. [2022], Gjerde et al. [202X]

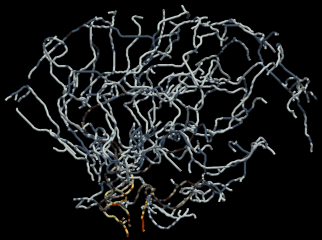

Human brain surface arteries (color: R_1)

Geometrically-reduced models accurately represent pulsatile flow in perivascular networks

Hodneland et al. [2019] (Vascular data), Olufsen [1999], Formaggia et al. [2003] Daversin-Catty et al. [2022], Gjerde et al. [202X]

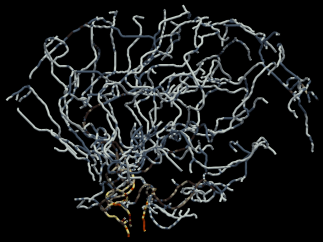

Human brain surface arteries (color: R_1)

Incompressible Stokes (3D)

Velocity v and pressure p s.t.

$$\partial_t v - \nu \nabla^2 v + \nabla p = 0 \quad \text{in } \Omega(t)$$
$$\nabla \cdot v = 0 \quad \text{in } \Omega(t)$$

where $\Omega(t) \overset{d}{\leftarrow\!\!\rightarrow} \Omega_0$ for $t > 0$.

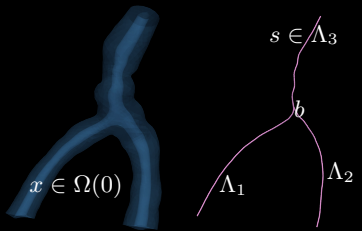

$v(x), p(x)$ $\quad$ $\hat{q}(s), \hat{p}(s)$

Geometrically-reduced models accurately represent pulsatile flow in perivascular networks

Hodneland et al. [2019] (Vascular data), Olufsen [1999], Formaggia et al. [2003] Daversin-Catty et al. [2022], Gjerde et al. [202X]

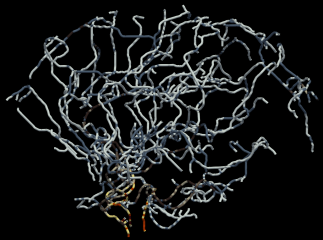

Human brain surface arteries (color: R_1)

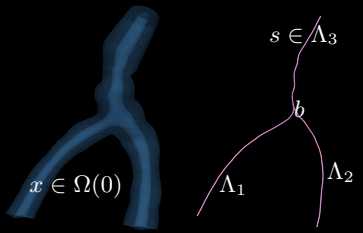

$v(x), p(x)$ $\quad$ $\hat{q}(s), \hat{p}(s)$

Incompressible Stokes (3D)

Velocity v and pressure p s.t.

$$\partial_t v - \nu \nabla^2 v + \nabla p = 0 \quad \text{in } \Omega(t)$$
$$\nabla \cdot v = 0 \quad \text{in } \Omega(t)$$

where $\Omega(t) \overset{d}{\leftarrow} \Omega_0$ for $t > 0$.

Model reduction concepts

PVS network $\Omega = \cup \Omega^i = \Omega^i(\Lambda^i)$, non-convex cross-sections $\Theta(s,t)$ with area $A^i(s,t)$.

Introduce

$$\hat{q}(s) = \int_{\Theta(s)} v \cdot \vec{s}$$

$$\hat{p}(s) = \int_{\Theta(s)} p$$

Assumptions: axial symmetry, radial motion, profiles, ...

Geometrically-reduced models accurately represent pulsatile flow in perivascular networks

Hodneland et al. [2019] (Vascular data), Olufsen [1999], Formaggia et al. [2003] Daversin-Catty et al. [2022], Gjerde et al. [202X]

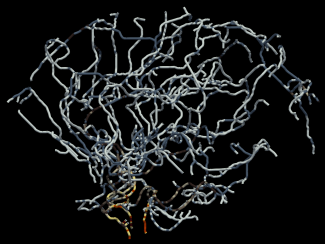

Human brain surface arteries (color: R_1)

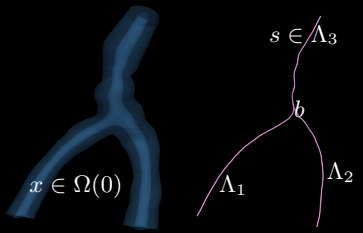

$v(x), p(x)$ $\quad$ $\hat{q}(s), \hat{p}(s)$

Incompressible Stokes (3D)

Velocity v and pressure p s.t.

$$\partial_t v - \nu \nabla^2 v + \nabla p = 0 \quad \text{in } \Omega(t)$$
$$\nabla \cdot v = 0 \quad \text{in } \Omega(t)$$

where $\Omega(t) \overset{d}{\leftarrow} \Omega_0$ for $t > 0$.

Model reduction concepts

PVS network $\Omega = \cup \Omega^i = \Omega^i(\Lambda^i)$, non-convex cross-sections $\Theta(s,t)$ with area $A^i(s,t)$.

Introduce

$$\hat{q}(s) = \int_{\Theta(s)} v \cdot \vec{s}$$
$$\hat{p}(s) = \int_{\Theta(s)} p$$

Assumptions: axial symmetry, radial motion, profiles, ...

Stokes–Brinkman flow (1D)

On each Λ^i, find flux $\hat{q}^i = \hat{q}^i(s,t)$ and pressure $\hat{p}^i = \hat{p}^i(s,t)$ s.t.

$$\partial_t \hat{q}^i + \nu \left(-\partial_{ss} \hat{q}^i + \alpha^i \hat{q}^i \right) + \partial_s \hat{p}^i = 0$$
$$\partial_s \hat{q}^i = -\partial_t A^i = 2\pi R_1 \partial_t d \cdot n$$

where $\alpha_i = \alpha_i(\Theta_i, v_{vp})$.

Conservation of flux and stress

At bifurcation points b:

$$\hat{q}^i(b) - \hat{q}^j(b) - \hat{q}^k(b) = 0$$
$$\hat{\sigma}^i(b) = \hat{\sigma}^j(b) = \hat{\sigma}^k(b)$$

with $A\hat{\sigma} = -\nu \partial_s \hat{q} + \hat{p}$.

Geometrically-reduced models accurately represent pulsatile flow in perivascular networks

Daversin-Catty et al. [2022], Gjerde et al. [202X]

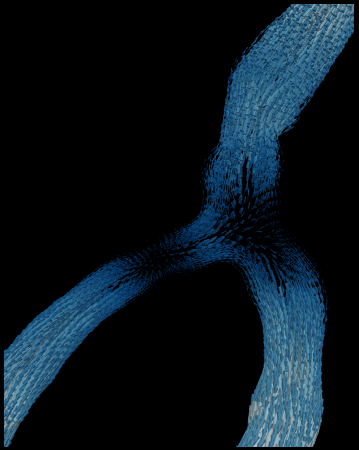

v

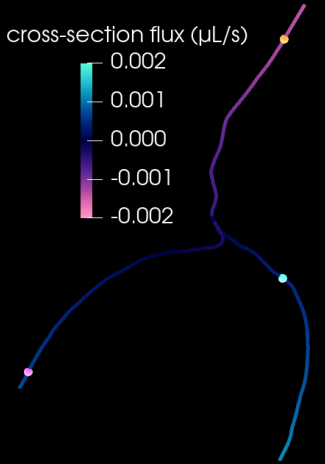

$\hat{q}$

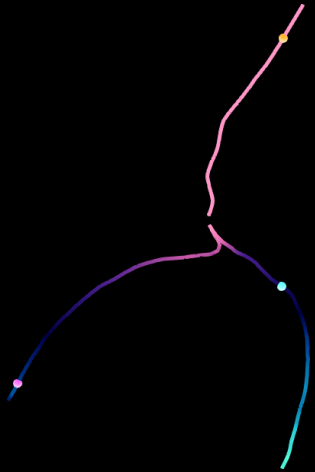

$\int_\Theta v \cdot \vec{s}$

Do graph topology affect the (finite element) stability of Stokes-Brinkman networks?

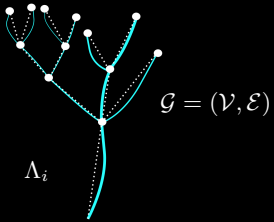

Boon et al. [2021], Gjerde et al. [202X]

Do graph topology affect the (finite element) stability of Stokes-Brinkman networks?

Boon et al. [2021], Gjerde et al. [202X]

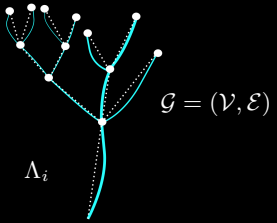

On each directed $\Lambda^i \in \mathcal{E}$, find the flux $\hat{q}^i$ and pressure $\hat{p}^i$ s.t.

$$\partial_t \hat{q}^i + \nu \left(-\partial_{ss} \hat{q}^i + \alpha^i \hat{q}^i \right) + \partial_s \hat{p}^i = 0$$

$$\partial_s \hat{q}^i = -\partial_t A^i = 2\pi R_1 \partial_t d \cdot n$$

Do graph topology affect the (finite element) stability of Stokes-Brinkman networks?

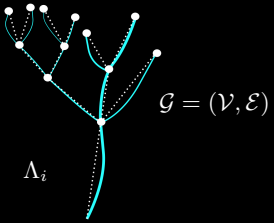

Boon et al. [2021], Gjerde et al. [202X]

On each directed $\Lambda^i \in \mathcal{E}$, find the flux $\hat{q}^i$ and pressure $\hat{p}^i$ s.t.

$$\partial_t \hat{q}^i + \nu \left(-\partial_{ss} \hat{q}^i + \alpha^i \hat{q}^i \right) + \partial_s \hat{p}^i = 0$$

$$\partial_s \hat{q}^i = -\partial_t A^i = \partial_t \hat{q}^i 2\pi R_1 \partial_t d \cdot n$$

Do graph topology affect the (finite element) stability of Stokes-Brinkman networks?

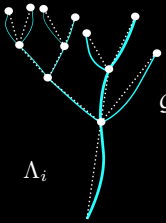

$\mathcal{G} = (\mathcal{V}, \mathcal{E})$

Λ_i

Boon et al. [2021], Gjerde et al. [202X]

On each directed $\Lambda^i \in \mathcal{E}$, find the flux $\hat{q}^i$ and pressure $\hat{p}^i$ s.t.

$$\partial_t \hat{q}^i + \nu \left(-\partial_{ss} \hat{q}^i + \alpha^i \hat{q}^i \right) + \partial_s \hat{p}^i = 0$$

$$\partial_s \hat{q}^i = -\partial_t A^i = \partial_t \hat{q}^i 2\pi R_1 \partial_t d \cdot n$$

Do graph topology affect the (finite element) stability of Stokes-Brinkman networks?

Boon et al. [2021], Gjerde et al. [202X]

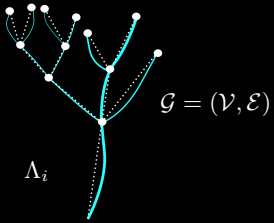

On each directed $\Lambda^i \in \mathcal{E}$, find the flux $\hat{q}^i$ and pressure $\hat{p}^i$ s.t.

$$\nu\alpha^i\hat{q}^i + \partial_s\hat{p}^i = -\nu\partial_s\partial_t A^i$$
$$\partial_s\hat{q}^i = -\partial_t A^i$$

Do graph topology affect the (finite element) stability of Stokes-Brinkman networks?

Boon et al. [2021], Gjerde et al. [202X]

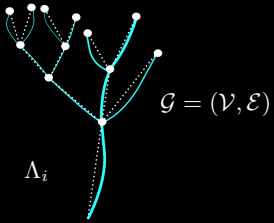

On each directed $\Lambda^i \in \mathcal{E}$, find the flux $\hat{q}^i$ and pressure $\hat{p}^i$ s.t.

$$\nu\alpha^i\hat{q}^i + \partial_s\hat{p}^i = -\nu\partial_s\partial_t A^i$$
$$\partial_s\hat{q}^i = -\partial_t A^i$$

Do graph topology affect the (finite element) stability of Stokes-Brinkman networks?

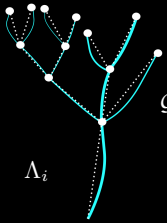

$\mathcal{G} = (\mathcal{V}, \mathcal{E})$

Λ_i

Boon et al. [2021], Gjerde et al. [202X]

On each directed $\Lambda^i \in \mathcal{E}$, find the flux $\hat{q}^i$ and pressure $\hat{p}^i$ s.t.

$$R^i \hat{q}^i + \partial_s \hat{p}^i = f^i$$
$$\partial_s \hat{q}^i = g^i$$

Do graph topology affect the (finite element) stability of Stokes-Brinkman networks?

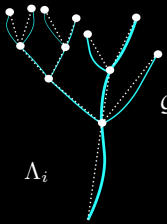

$\mathcal{G} = (\mathcal{V}, \mathcal{E})$

Λ_i

Boon et al. [2021], Gjerde et al. [202X]

On each directed $\Lambda^i \in \mathcal{E}$, find the flux q^i and pressure p^i s.t.

$$R^i q^i + \partial_s p^i = f^i$$
$$\partial_s q^i = g^i$$

Do graph topology affect the (finite element) stability of Stokes-Brinkman networks?

Boon et al. [2021], Gjerde et al. [202X]

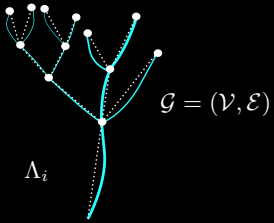

On each directed $\Lambda^i \in \mathcal{E}$, find the flux q^i and pressure p^i s.t.

$$R^i q^i + \partial_s p^i = f^i$$
$$\partial_s q^i = g^i$$

At $b \in \mathcal{V}$ with incident edges $\mathcal{E}(b)$

$$[\![q]\!](b) = 0$$
$$p^i(b) = p^j(b) \qquad \Lambda^i, \Lambda^j \in \mathcal{E}(b)$$

Berkolaiko and Kuchment [2013], Arioli and Benzi [2018]

Do graph topology affect the (finite element) stability of Stokes-Brinkman networks?

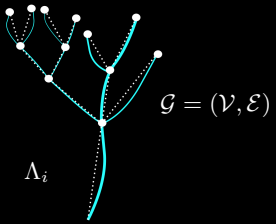

On each directed $\Lambda^i \in \mathcal{E}$, find the flux q^i and pressure p^i s.t.

$$R^i q^i + \partial_s p^i = f^i$$
$$\partial_s q^i = g^i$$

At $b \in \mathcal{V}$ with incident edges $\mathcal{E}(b)$

$$[\![q]\!](b) = 0$$
$$p^i(b) = p^j(b) \qquad \Lambda^i, \Lambda^j \in \mathcal{E}(b)$$

Berkolaiko and Kuchment [2013], Arioli and Benzi [2018]

Dual variational form $*$

Find $(q, p, z) \in X = Q \times P \times Z$ s. t.

$$(Rq, \psi)_{\mathcal{E}} - (\partial_s \psi, p)_{\mathcal{E}} - ([\![\psi]\!], z)_{\mathcal{V}} = (f, \psi)_{\mathcal{E}}$$
$$(\partial_s q, \phi)_{\mathcal{E}} + ([\![q]\!], w)_{\mathcal{V}} = (g, \phi)_{\mathcal{E}}$$

for all $(\psi, \phi, w) \in X$.

with $X = H(\nabla\cdot, \mathcal{G}) \times L^2(\mathcal{E}) \times L^2(\mathcal{V})$.

Boon et al. [2021], Gjerde et al. [202X]

Do graph topology affect the (finite element) stability of Stokes-Brinkman networks?

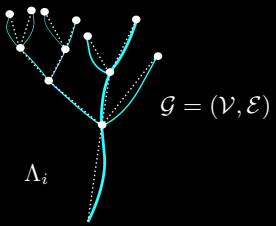

On each directed $\Lambda^i \in \mathcal{E}$, find the flux q^i and pressure p^i s.t.

$$R^i q^i + \partial_s p^i = f^i$$
$$\partial_s q^i = g^i$$

At $b \in \mathcal{V}$ with incident edges $\mathcal{E}(b)$

$$[\![q]\!](b) = 0$$
$$p^i(b) = p^j(b) \qquad \Lambda^i, \Lambda^j \in \mathcal{E}(b)$$

Berkolaiko and Kuchment [2013], Arioli and Benzi [2018]

Boon et al. [2021], Gjerde et al. [202X]

Dual variational form $*$

Find $(q, p, z) \in X = Q \times P \times Z$ s. t.

$$(Rq, \psi)_{\mathcal{E}} - (\partial_s \psi, p)_{\mathcal{E}} - ([\![\psi]\!], z)_{\mathcal{V}} = (f, \psi)_{\mathcal{E}}$$
$$(\partial_s q, \phi)_{\mathcal{E}} + ([\![q]\!], w)_{\mathcal{V}} = (g, \phi)_{\mathcal{E}}$$

for all $(\psi, \phi, w) \in X$.

with $X = H(\nabla\cdot, \mathcal{G}) \times L^2(\mathcal{E}) \times L^2(\mathcal{V})$.

Natural norms?

$$\|q\|_Q^2 = \|q\|_{L^2(\mathcal{E})}^2 + \|\partial_s q\|_{L^2(\mathcal{E})}^2 + \|[\![q]\!]\|_{L^2(\mathcal{V})}^2$$
$$\|p\|_P^2 = \|p\|_{L^2(\mathcal{E})}^2$$
$$\|z\|_Z^2 = \|z\|_{L^2(\mathcal{V})}^2$$

Do graph topology affect the (finite element) stability of Stokes-Brinkman networks?

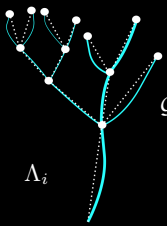

On each directed $\Lambda^i \in \mathcal{E}$, find the flux q^i and pressure p^i s.t.

$$R^i q^i + \partial_s p^i = f^i$$
$$\partial_s q^i = g^i$$

At $b \in \mathcal{V}$ with incident edges $\mathcal{E}(b)$

$$[\![q]\!](b) = 0$$
$$p^i(b) = p^j(b) \qquad \Lambda^i, \Lambda^j \in \mathcal{E}(b)$$

Berkolaiko and Kuchment [2013], Arioli and Benzi [2018]

Dual variational form $*$

Find $(q, p, z) \in X = Q \times P \times Z$ s. t.

$$(Rq, \psi)_{\mathcal{E}} - (\partial_s \psi, p)_{\mathcal{E}} - ([\![\psi]\!], z)_{\mathcal{V}} = (f, \psi)_{\mathcal{E}}$$
$$(\partial_s q, \phi)_{\mathcal{E}} + ([\![q]\!], w)_{\mathcal{V}} = (g, \phi)_{\mathcal{E}}$$

for all $(\psi, \phi, w) \in X$.

with $X = H(\nabla\cdot, \mathcal{G}) \times L^2(\mathcal{E}) \times L^2(\mathcal{V})$.

Natural norms?

$$\|q\|_Q^2 = \|q\|_{L^2(\mathcal{E})}^2 + \|\partial_s q\|_{L^2(\mathcal{E})}^2 + \|[\![q]\!]\|_{L^2(\mathcal{V})}^2$$
$$\|p\|_P^2 = \|p\|_{L^2(\mathcal{E})}^2$$
$$\|z\|_Z^2 = \|z\|_{L^2(\mathcal{V})}^2$$

Boon et al. [2021], Gjerde et al. [202X]

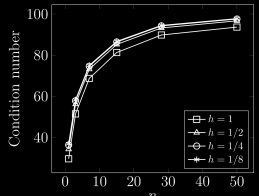

Not robust in $n = |\mathcal{V}|$

Do graph topology affect the (finite element) stability of Stokes-Brinkman networks?

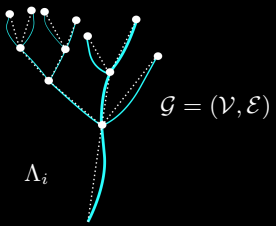

On each directed $\Lambda^i \in \mathcal{E}$, find the flux q^i and pressure p^i s.t.

$$R^i q^i + \partial_s p^i = f^i$$
$$\partial_s q^i = g^i$$

At $b \in \mathcal{V}$ with incident edges $\mathcal{E}(b)$

$$[\![q]\!](b) = 0$$
$$p^i(b) = p^j(b) \qquad \Lambda^i, \Lambda^j \in \mathcal{E}(b)$$

Berkolaiko and Kuchment [2013], Arioli and Benzi [2018]

Boon et al. [2021], Gjerde et al. [202X]

Dual variational form $*$

Find $(q, p, z) \in X = Q \times P \times Z$ s. t.

$$(Rq, \psi)_{\mathcal{E}} - (\partial_s \psi, p)_{\mathcal{E}} - ([\![\psi]\!], z)_{\mathcal{V}} = (f, \psi)_{\mathcal{E}}$$
$$(\partial_s q, \phi)_{\mathcal{E}} + ([\![q]\!], w)_{\mathcal{V}} = (g, \phi)_{\mathcal{E}}$$

for all $(\psi, \phi, w) \in X$.

with $X = H(\nabla\cdot, \mathcal{G}) \times L^2(\mathcal{E}) \times L^2(\mathcal{V})$.

Weighted norms †

$$\|q\|_Q^2 = \|q\|_{L^2(\mathcal{E})}^2 + \|\ell \partial_s q\|_{L^2(\mathcal{E})}^2 + \|L_\ell [\![q]\!]\|_{L^2(\mathcal{V})}^2$$
$$\|p\|_P^2 = \|\ell^{-1} p\|_{L^2(\mathcal{E})}^2$$
$$\|z\|_Z^2 = \|L_\ell^{-1} z\|_{L^2(\mathcal{V})}^2$$

for $\ell = \sum_i |\Lambda_i|$, L_ℓ averaged local lengths

Do graph topology affect the (finite element) stability of Stokes-Brinkman networks?

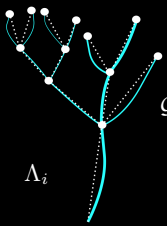

On each directed $\Lambda^i \in \mathcal{E}$, find the flux q^i and pressure p^i s.t.

$$R^i q^i + \partial_s p^i = f^i$$
$$\partial_s q^i = g^i$$

At $b \in \mathcal{V}$ with incident edges $\mathcal{E}(b)$

$$[\![q]\!](b) = 0$$
$$p^i(b) = p^j(b) \qquad \Lambda^i, \Lambda^j \in \mathcal{E}(b)$$

Berkolaiko and Kuchment [2013], Arioli and Benzi [2018]

Dual variational form $*$

Find $(q, p, z) \in X = Q \times P \times Z$ s. t.

$$(Rq, \psi)_{\mathcal{E}} - (\partial_s \psi, p)_{\mathcal{E}} - ([\![\psi]\!], z)_{\mathcal{V}} = (f, \psi)_{\mathcal{E}}$$
$$(\partial_s q, \phi)_{\mathcal{E}} + ([\![q]\!], w)_{\mathcal{V}} = (g, \phi)_{\mathcal{E}}$$

for all $(\psi, \phi, w) \in X$.

with $X = H(\nabla\cdot, \mathcal{G}) \times L^2(\mathcal{E}) \times L^2(\mathcal{V})$.

Weighted norms †

$$\|q\|_Q^2 = \|q\|_{L^2(\mathcal{E})}^2 + \|\ell \partial_s q\|_{L^2(\mathcal{E})}^2 + \|L_\ell [\![q]\!]\|_{L^2(}^2$$
$$\|p\|_P^2 = \|\ell^{-1} p\|_{L^2(\mathcal{E})}^2$$
$$\|z\|_Z^2 = \|L_\ell^{-1} z\|_{L^2(\mathcal{V})}^2$$

for $\ell = \sum_i |\Lambda_i|$, L_ℓ averaged local lengths

Boon et al. [2021], Gjerde et al. [202X]

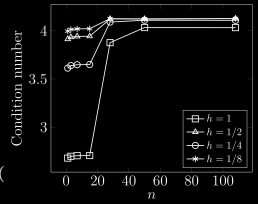

Uniform in $n = |\mathcal{V}|$

[Perivascular spaces, NIH Research Matters Graphics, Maiken Nedergaard (Oct 28 2013)]

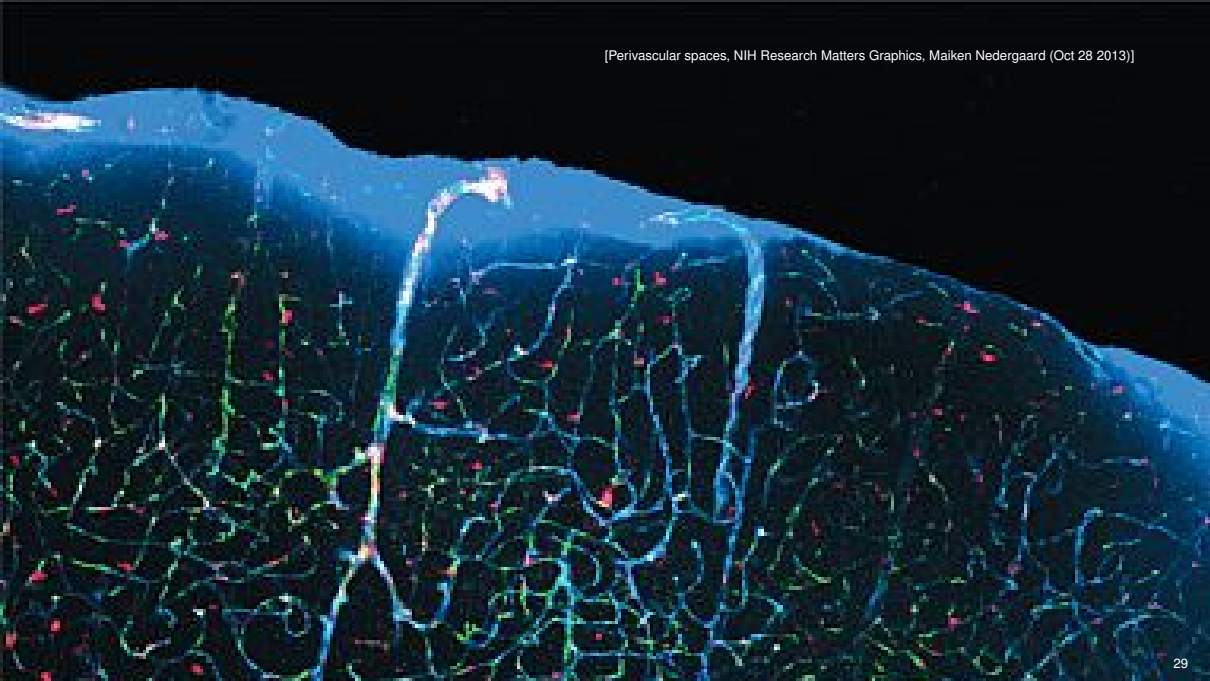

MRI reveals human brain-wide tracer enhancement and clearance

Ringstad et al. [2017, 2018]

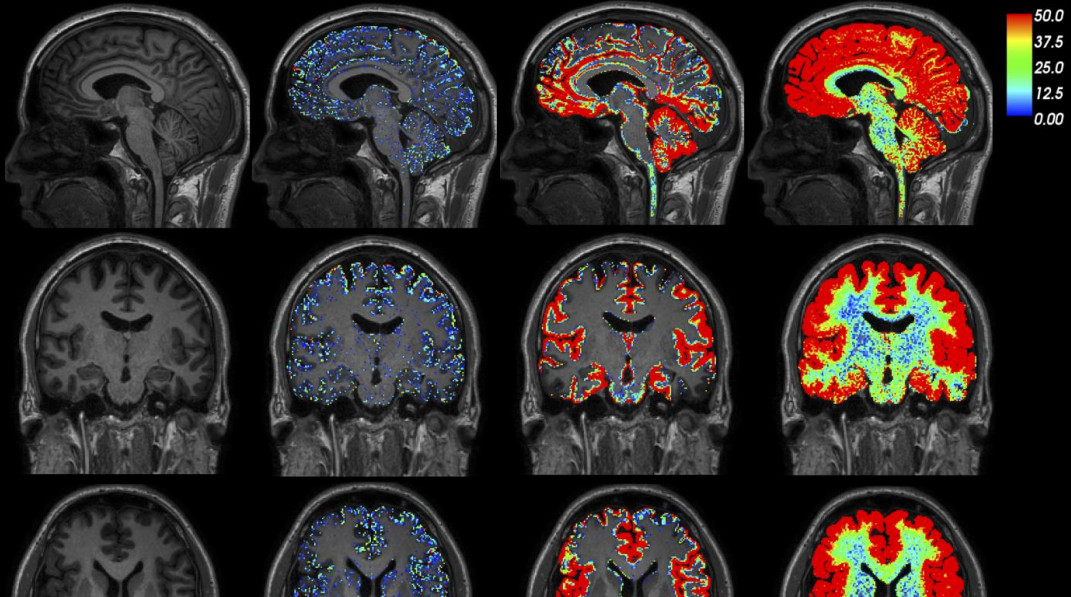

The D'A-Q. 3D-1D equations are well-posed in weighted Sobolev spaces (only)

[D'Angelo and Quarteroni (2008), Drelichman et al (2020)]

Find $u : \Omega \to \mathbb{R}$ and $\hat{u} : \Lambda \to \mathbb{R}$ such that

$$-\nabla\cdot(k\,\nabla u) - \beta(\hat{u} - \bar{u})\delta_\Lambda = 0 \quad \text{in } \Omega, \qquad \text{(5a)}$$

$$-\partial_s(\hat{k}\partial_s\hat{u}) + \beta(\hat{u} - \bar{u}) = 0 \quad \text{in } \Lambda, \qquad \text{(5b)}$$

where $\bar{u}$ is a circumferential average:

$$\bar{u}(s) = (2\pi R)^{-1} \int_0^{2\pi} u(s, R, \theta)\,\mathrm{d}\theta, \quad s \in \Lambda.$$

The D'A-Q. 3D-1D equations are well-posed in weighted Sobolev spaces (only)

[D'Angelo and Quarteroni (2008), Drelichman et al (2020)]

Find $u : \Omega \to \mathbb{R}$ and $\hat{u} : \Lambda \to \mathbb{R}$ such that

$$-\nabla\cdot(k\,\nabla u) - \beta(\hat{u} - \bar{u})\delta_\Lambda = 0 \quad \text{in } \Omega, \qquad (5a)$$

$$-\partial_s(\hat{k}\partial_s\hat{u}) + \beta(\hat{u} - \bar{u}) = 0 \quad \text{in } \Lambda, \qquad (5b)$$

where $\bar{u}$ is a circumferential average:

$$\bar{u}(s) = (2\pi R)^{-1} \int_0^{2\pi} u(s, R, \theta)\,\mathrm{d}\theta, \quad s \in \Lambda.$$

Key idea: Analyze the decoupled elliptic problem with (low regularity) line measure terms: given $\hat{u}$, find $u : \Omega \to \mathbb{R}$ solving (5a).

[Stampacchia (1965), Brezis and Strauss (1973), Scott (1973), Casas (1985)]

What are U, V such that $u \in U$ solves

$$(k\,\nabla u, \nabla v)_\Omega + (\beta\bar{u}, v)_\Lambda = (\beta\hat{u}, v)_\Lambda, \qquad (6)$$

for all $v \in V$?

The D'A-Q. 3D-1D equations are well-posed in weighted Sobolev spaces (only)

[D'Angelo and Quarteroni (2008), Drelichman et al (2020)]

Find $u : \Omega \to \mathbb{R}$ and $\hat{u} : \Lambda \to \mathbb{R}$ such that

$$-\nabla\cdot(k\,\nabla u) - \beta(\hat{u} - \bar{u})\delta_\Lambda = 0 \quad \text{in } \Omega, \qquad (5a)$$

$$-\partial_s(\hat{k}\partial_s\hat{u}) + \beta(\hat{u} - \bar{u}) = 0 \quad \text{in } \Lambda, \qquad (5b)$$

where $\bar{u}$ is a circumferential average:

$$\bar{u}(s) = (2\pi R)^{-1} \int_0^{2\pi} u(s, R, \theta)\,\mathrm{d}\theta, \quad s \in \Lambda.$$

Key idea: Analyze the decoupled elliptic problem with (low regularity) line measure terms: given $\hat{u}$, find $u : \Omega \to \mathbb{R}$ solving (5a).

[Stampacchia (1965), Brezis and Strauss (1973), Scott (1973), Casas (1985)]

What are U, V such that $u \in U$ solves

$$(k\,\nabla u, \nabla v)_\Omega + (\beta\bar{u}, v)_\Lambda = (\beta\hat{u}, v)_\Lambda, \qquad (6)$$

for all $v \in V$? (Not $H^1(\Omega)$!)

The D'A-Q. 3D-1D equations are well-posed in weighted Sobolev spaces (only)

[D'Angelo and Quarteroni (2008), Drelichman et al (2020)]

Find $u : \Omega \to \mathbb{R}$ and $\hat{u} : \Lambda \to \mathbb{R}$ such that

$$-\nabla\cdot(k\,\nabla u) - \beta(\hat{u} - \bar{u})\delta_\Lambda = 0 \quad \text{in } \Omega, \qquad (5a)$$

$$-\partial_s(\hat{k}\partial_s\hat{u}) + \beta(\hat{u} - \bar{u}) = 0 \quad \text{in } \Lambda, \qquad (5b)$$

where $\bar{u}$ is a circumferential average:

$$\bar{u}(s) = (2\pi R)^{-1} \int_0^{2\pi} u(s, R, \theta)\,\mathrm{d}\theta, \quad s \in \Lambda.$$

Introduce weighted Sobolev spaces $\alpha \in (-1, 1)$:

$$L^2_\alpha(\Omega) = \{u \,|\, \mathrm{dist}^\alpha u \in L^2(\Omega), \mathrm{dist}(x) = \mathrm{dist}(x, \Lambda)\}$$

$$H^1_\alpha(\Omega) = \{u \in L^2_\alpha(\Omega) \mid \nabla u \in L^2_\alpha(\Omega)^d\}$$

$$H^1_{-\alpha}(\Omega) \subset H^1(\Omega) \subset H^1_\alpha(\Omega), \quad \alpha \in (0, 1)$$

Key idea: Analyze the decoupled elliptic problem with (low regularity) line measure terms: given $\hat{u}$, find $u : \Omega \to \mathbb{R}$ solving (5a).

[Stampacchia (1965), Brezis and Strauss (1973), Scott (1973), Casas (1985)]

What are U, V such that $u \in U$ solves

$$(k\,\nabla u, \nabla v)_\Omega + (\beta\bar{u}, v)_\Lambda = (\beta\hat{u}, v)_\Lambda, \qquad (6)$$

for all $v \in V$? (Not $H^1(\Omega)$!)

Theorem (Well-posedness, D'A & Q (2008))

There exists $0 < \alpha < 1$ *such that* (6) *with* $U = \mathring{H}^1_\alpha(\Omega)$, $V = H^1_{-\alpha}(\Omega)$ *is well-posed.*

Proof.

Via a generalized Lax-Milgram theorem, continuity and coercivity in the weighted spaces. □

Coupling via the interface surface gives well-posedness in standard Sobolev spaces

[Köppl, Vidotto, Wohlmuth, Zunino (2018) ($d = 2$)]

Consider the curve Λ, the cylinder surface Γ, and the embedding domain $\Omega \subset \mathbb{R}^d$.

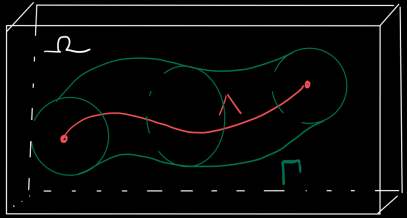

Coupling via the interface surface gives well-posedness in standard Sobolev spaces

[Köppl, Vidotto, Wohlmuth, Zunino (2018) ($d = 2$)]

Consider the curve Λ, the cylinder surface Γ, and the embedding domain $\Omega \subset \mathbb{R}^d$.

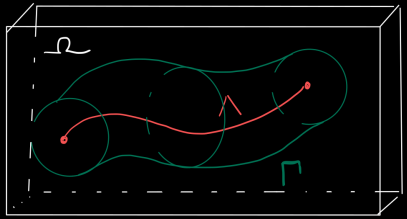

New idea: Analyze the decoupled 3D problem with (not line but) surface measure terms: given $\tilde{u} : \Gamma \to \mathbb{R}$, find $u : \Omega \to \mathbb{R}$ such that

$$-\nabla\cdot(k\,\nabla\,u) - \beta(\tilde{u} - \bar{u})\delta_\Gamma = 0 \quad \text{in } \Omega.$$

What are U, V such that $u \in U$ solves

$$(k\,\nabla\,u, \nabla\,v)_\Omega + (\beta\bar{u}, v)_\Gamma = (\beta\tilde{u}, v)_\Gamma, \qquad (7)$$

for all $v \in V$?

Coupling via the interface surface gives well-posedness in standard Sobolev spaces

[Köppl, Vidotto, Wohlmuth, Zunino (2018) ($d = 2$)]

Consider the curve Λ, the cylinder surface Γ, and the embedding domain $\Omega \subset \mathbb{R}^d$.

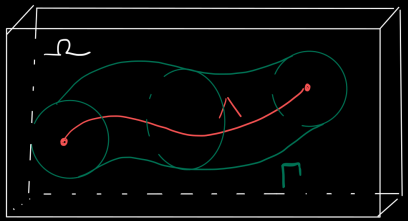

New idea: Analyze the decoupled 3D problem with (not line but) surface measure terms: given $\tilde{u} : \Gamma \to \mathbb{R}$, find $u : \Omega \to \mathbb{R}$ such that

$$-\nabla\cdot(k\,\nabla u) - \beta(\tilde{u} - \bar{u})\delta_\Gamma = 0 \quad \text{in } \Omega.$$

What are U, V such that $u \in U$ solves

$$(k\,\nabla u, \nabla v)_\Omega + (\beta\bar{u}, v)_\Gamma = (\beta\tilde{u}, v)_\Gamma, \qquad (7)$$

for all $v \in V$?

Theorem (Well-posedness, KVWZ (2018))

For R sufficiently small, (7) *is well-posed for* $U \times V = H_0^1(\Omega) \times H^{-1}(\Omega)$*, and*

$$u \in H_0^1(\Omega) \cap H^{\frac{3}{2}-\epsilon}$$

Proof.

Lax-Milgram with tailored trace inequality. □

Coupling via the interface surface gives well-posedness in standard Sobolev spaces

[Köppl, Vidotto, Wohlmuth, Zunino (2018) ($d = 2$)]

Consider the curve Λ, the cylinder surface Γ, and the embedding domain $\Omega \subset \mathbb{R}^d$.

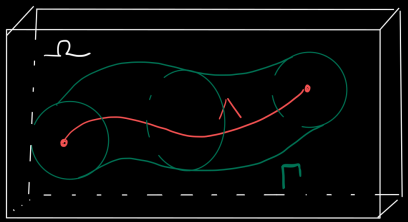

Q1 Existence and uniqueness of solutions?

Q2 How are these equations derived?

Q3 What is the modelling error?

Q4 What is the approximation error?

New idea: Analyze the decoupled 3D problem with (not line but) surface measure terms: given $\tilde{u} : \Gamma \to \mathbb{R}$, find $u : \Omega \to \mathbb{R}$ such that

$$-\nabla\cdot(k\,\nabla u) - \beta(\tilde{u} - \bar{u})\delta_\Gamma = 0 \quad \text{in } \Omega.$$

What are U, V such that $u \in U$ solves

$$(k\,\nabla u, \nabla v)_\Omega + (\beta\bar{u}, v)_\Gamma = (\beta\tilde{u}, v)_\Gamma, \qquad (7)$$

for all $v \in V$?

Theorem (Well-posedness, KVWZ (2018))

For R sufficiently small, (7) *is well-posed for* $U \times V = H_0^1(\Omega) \times H^{-1}(\Omega)$*, and*

$$u \in H_0^1(\Omega) \cap H^{\frac{3}{2}-\epsilon}$$

Proof.

Lax-Milgram with tailored trace inequality. □

3D-1D modelling of molecular transport in perivascular pathways and brain tissue

Masri et al. [2024, 202X]



Tissue $\Omega \in \mathbb{R}^3$

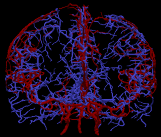

Vessels $\Lambda = \cup_i \Lambda_i$

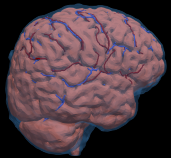

Hodneland et al. [2019] (Data set)

3D-1D modelling of molecular transport in perivascular pathways and brain tissue

Masri et al. [2024, 202X]

Tissue $\Omega \in \mathbb{R}^3$

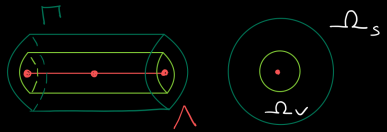

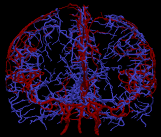

Vessels $\Lambda = \cup_i \Lambda_i$

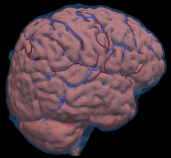

Hodneland et al. [2019] (Data set)

3D-1D modelling of molecular transport in perivascular pathways and brain tissue

Masri et al. [2024, 202X]

Tissue $\Omega \in \mathbb{R}^3$

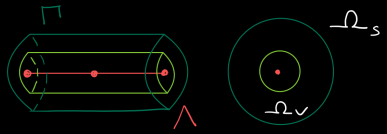



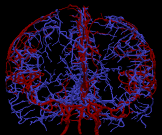

Vessels $\Lambda = \cup_i \Lambda_i$

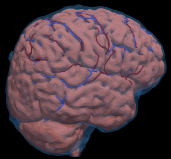

Hodneland et al. [2019] (Data set)

3D-3D transport and exchange

Find concentrations $c_r(t) : \Omega_r \to \mathbb{R}$ s.t.

$$\partial_t c_r - \nabla \cdot (D_r \nabla c_r - u_r c_r) = 0 \qquad \text{in } \Omega_r(t)$$

and across $\Gamma(t)$:

$$-(D_v \nabla c_v - \tilde{u}_v c_v) \cdot n_v - \zeta(c_v - c_s) = 0$$

3D-1D modelling of molecular transport in perivascular pathways and brain tissue

Masri et al. [2024, 202X]

Tissue $\Omega \in \mathbb{R}^3$

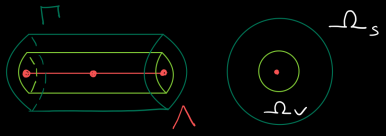

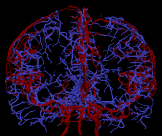

Vessels $\Lambda = \cup_i \Lambda_i$

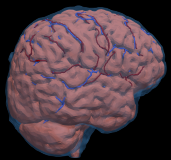

Hodneland et al. [2019] (Data set)

3D-3D transport and exchange

Find concentrations $c_r(t) : \Omega_r \to \mathbb{R}$ s.t.

$$\partial_t c_r - \nabla \cdot (D_r \nabla c_r - u_r c_r) = 0 \qquad \text{in } \Omega_r(t)$$

and across $\Gamma(t)$:

$$-(D_v \nabla c_v - \tilde{u}_v c_v) \cdot n_v - \zeta(c_v - c_s) = 0$$

Model reduction tools

Cross-section average

$$\langle c \rangle(s) \equiv \frac{1}{A(s)} \int_{\Theta(s)} c$$

Perimeter average

$$\bar{f}(s) \equiv \frac{1}{P(s)} \int_{\partial\Theta_2(s)} f$$

3D-1D coupling via the KVWZ trick.

3D-1D modelling of molecular transport in perivascular pathways and brain tissue

Masri et al. [2024, 202X]

Tissue $\Omega \in \mathbb{R}^3$

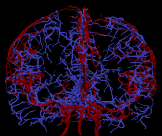

Vessels $\Lambda = \cup_i \Lambda_i$

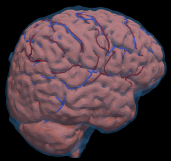

Hodneland et al. [2019] (Data set)

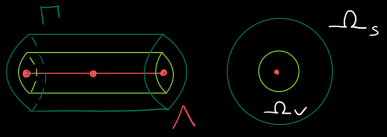

3D-3D transport and exchange

Find concentrations $c_r(t) : \Omega_r \to \mathbb{R}$ s.t.

$$\partial_t c_r - \nabla\cdot(D_r \nabla c_r - u_r c_r) = 0 \qquad \text{in } \Omega_r(t)$$

and across $\Gamma(t)$:

$$-(D_v \nabla c_v - \tilde{u}_v c_v)\cdot n_v - \zeta(c_v - c_s) = 0$$

3D-1D

Find $c(t) : \Omega \to \mathbb{R}$, $\hat{c}(t) : \Lambda \to \mathbb{R}$ s.t.

$$\partial_t c - \nabla\cdot(\mathcal{E}D \nabla c - \mathcal{E}uc) + \zeta(\bar{c} - \hat{c})\delta_\Gamma = 0,$$
$$\partial_t(A\hat{c}) - \partial_s\left(DA\partial_s\hat{c} - A\langle u\rangle\hat{c}\right) + P\zeta(\hat{c} - \bar{c}) = 0,$$

in Ω and Λ, respectively.

Model reduction tools

Cross-section average

$$\langle c\rangle(s) \equiv \frac{1}{A(s)}\int_{\Theta(s)} c$$

Perimeter average

$$\bar{f}(s) \equiv \frac{1}{P(s)}\int_{\partial\Theta_2(s)} f$$

3D-1D coupling via the KVWZ trick.

The 3D-3D and 3D-1D perivascular-tissue transport equations are well-posed

Masri et al. [2024, 202X]

Tissue $\Omega \in \mathbb{R}^3$

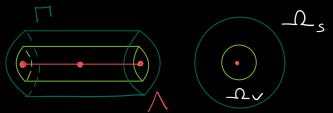

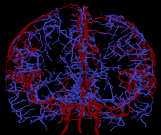

Vessels $\Lambda = \cup_i \Lambda_i$

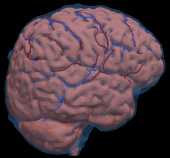

Hodneland et al. [2019] (Data set)

The 3D-3D and 3D-1D perivascular-tissue transport equations are well-posed

Masri et al. [2024, 202X]

Tissue $\Omega \in \mathbb{R}^3$

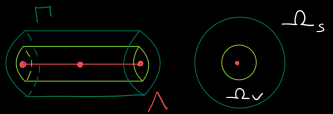

3D-1D transport and exchange

Find $c(t) : \Omega \to \mathbb{R}$, $\hat{c}(t) : \Lambda \to \mathbb{R}$ s.t.

$$\partial_t c - \nabla \cdot (\mathcal{E} D \nabla c - \mathcal{E} u c) + \zeta(\bar{c} - \hat{c})\delta_\Gamma = 0,$$
$$\partial_t (A\hat{c}) - \partial_s \left(DA\partial_s \hat{c} - A\langle u \rangle \hat{c} \right) + P\zeta(\hat{c} - \bar{c}) = 0,$$

in Ω and Λ, respectively.

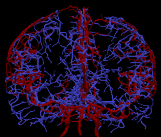

Vessels $\Lambda = \cup_i \Lambda_i$

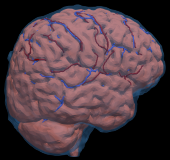

Hodneland et al. [2019] (Data set)

The 3D-3D and 3D-1D perivascular-tissue transport equations are well-posed

Masri et al. [2024, 202X]

Tissue $\Omega \in \mathbb{R}^3$

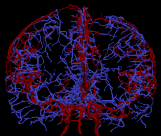

Vessels $\Lambda = \cup_i \Lambda_i$

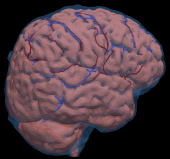

Hodneland et al. [2019] (Data set)

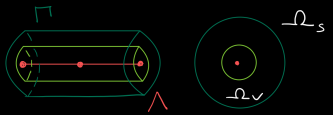

3D-1D transport and exchange

Find $c(t) : \Omega \to \mathbb{R}$, $\hat{c}(t) : \Lambda \to \mathbb{R}$ s.t.

$$\partial_t c - \nabla\cdot(\mathcal{E}D\,\nabla\, c - \mathcal{E}uc) + \zeta(\bar{c} - \hat{c})\delta_\Gamma = 0,$$
$$\partial_t(A\hat{c}) - \partial_s\left(DA\partial_s\hat{c} - A\langle u\rangle\hat{c}\right) + P\zeta(\hat{c} - \bar{c}) = 0,$$

in Ω and Λ, respectively.

Theorem

Assuming uniformly bounded data, the (variational) 3D-1D transport equations are well-posed over

$$\{c \in L^2(0,T,H_0^1(\Omega)), \partial_t c \in L^2(0,T,H^{-1}(\Omega))\}\times$$
$$\{\hat{c} \in L^2(0,T,H_A^1(\Lambda)), \partial_t\hat{c} \in L^2(0,T,H_A^{-1}(\Lambda))\}$$

Will the 3D-3D and 3D-1D perivascular transport models agree for infinitely thin vessels?

Masri et al. [2024]

Theorem (Model error in the perivascular space)

Let c_v, c_s be weak solutions to the coupled 3D-3D perivascular transport problem and assume that $c_v(0) \in H^1(\Omega_v)$. Let $c, \hat{c}$ be the weak solutions to the reduced coupled 3D-1D perivascular transport problem.

Then, for $\epsilon = \max \operatorname{diam} \Theta(s,t)$

$$\begin{aligned}\|c_v - \hat{c}\|_{L^2(0,T;L^2(\Omega_v))} &\lesssim \epsilon + \epsilon^{1/2} + (\epsilon|\ln\epsilon|)^{1/2} \\ &\quad + \|u_{v,r}, u_{v,\theta}\| + \max \partial_s |R_1, R_2|\end{aligned}$$

Here, the inequality constant(s) depend on the data, parameters and the solutions $c, \hat{c}$, and c_s, but are bounded independently of ϵ.

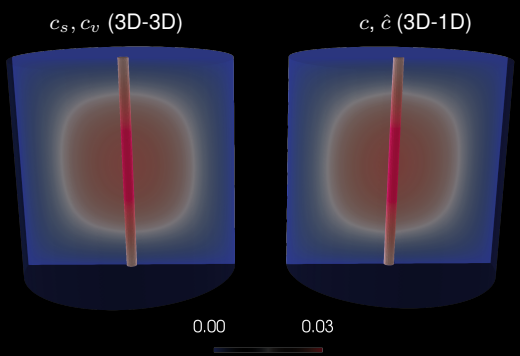

($h_{\max} \approx 0.02$)

2ϵ	E_v	rate
0.1	4.39×10^{-4}	-
0.05	5.26×10^{-5}	3.06
0.025	1.41×10^{-5}	1.90
0.0125	7.90×10^{-6}	0.84

MRI highlights need for individualized treatment of brain diseases

Ringstad et al. [2018]

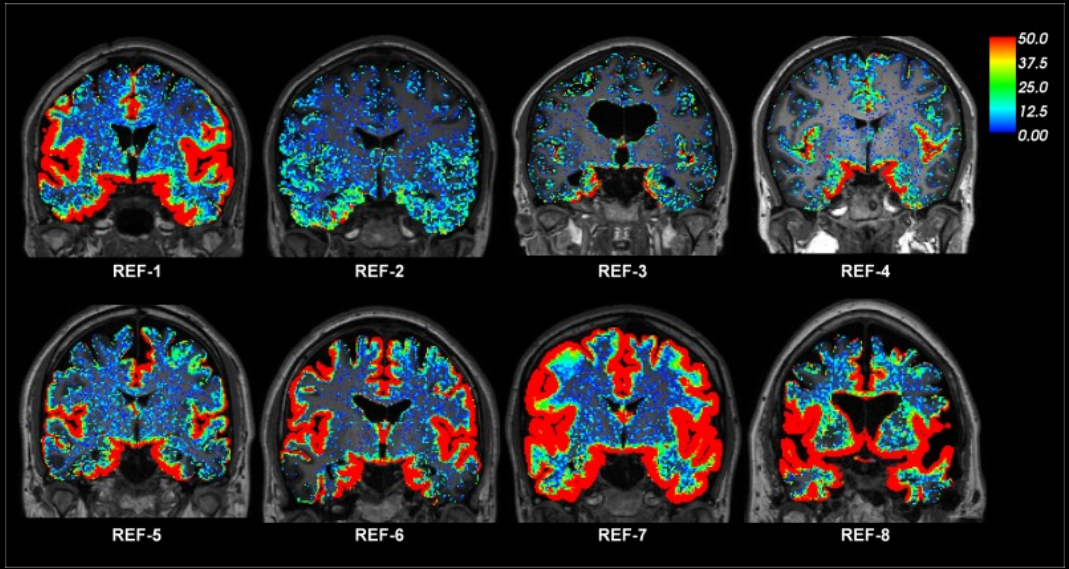

K. G. Jebsen Centre for Brain Fluid Research targeting new diagnostics for dementia disorders and more precise treatment of brain cancer (2024–2029)

Personalized in-silico predictions of molecular transport in the human intracranial space

Causemann et al. [2022], Hornkjøl et al. [2022], Gjerde et al. [2023], Masri et al. [2024, 202X]

Brain++ $\Omega \in \mathbb{R}^3$

Find $c(t) : \Omega \to \mathbb{R}$, $\hat{c}(t) : \Lambda \to \mathbb{R}$ s.t.

$$\partial_t c - \nabla \cdot (\mathcal{E} D \nabla c - \mathcal{E} u c) + \zeta(\bar{c} - \hat{c})\delta_\Gamma = 0$$
$$\partial_t (A\hat{c}) - \partial_s \left(DA\partial_s \hat{c} - A\hat{u}\hat{c} \right) + P\zeta(\hat{c} - \bar{c}) = 0$$

in Ω and Λ, respectively.

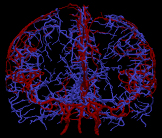

Vessels $\Lambda = \cup_i \Lambda_i$

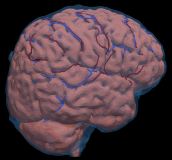

Personalized in-silico predictions of molecular transport in the human intracranial space

Causemann et al. [2022], Hornkjøl et al. [2022], Gjerde et al. [2023], Masri et al. [2024, 202X]

Brain++ $\Omega \in \mathbb{R}^3$

Find $c(t) : \Omega \to \mathbb{R}$, $\hat{c}(t) : \Lambda \to \mathbb{R}$ s.t.

$$\partial_t c - \nabla \cdot (\mathcal{E} D \nabla c - \mathcal{E} u c) + \zeta(\bar{c} - \hat{c})\delta_\Gamma = 0$$
$$\partial_t (A\hat{c}) - \partial_s \left(DA\partial_s \hat{c} - A\hat{u}\hat{c} \right) + P\zeta(\hat{c} - \bar{c}) = 0$$

in Ω and Λ, respectively.

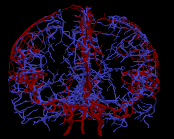

Vessels $\Lambda = \cup_i \Lambda_i$

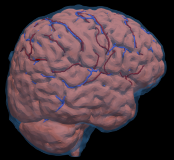

Computational fluid dynamics to inform transport models

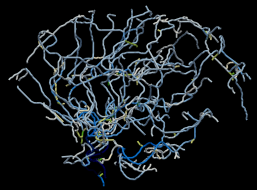

PVS flow $\hat{u}$ from vasomotion

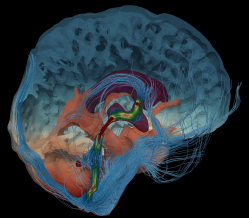

Flow u from CSF production

In-silico molecular transport in the human intracranial space after intrathecal injection (24h)

Masri et al. [202X]

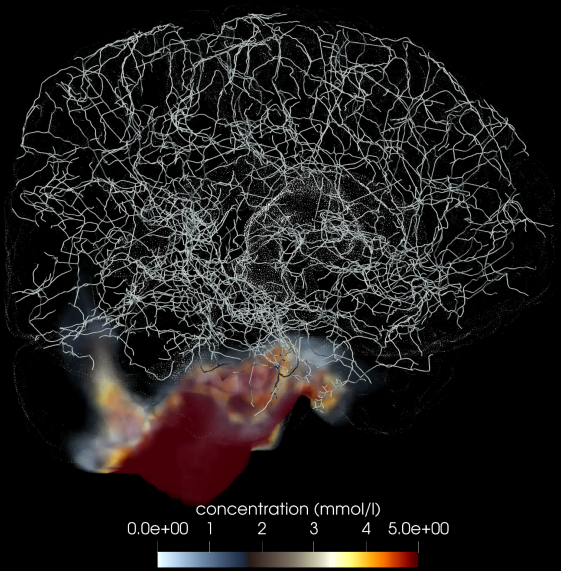

Final remarks

Mathematical modeling of the human brain: from MRI to FEM

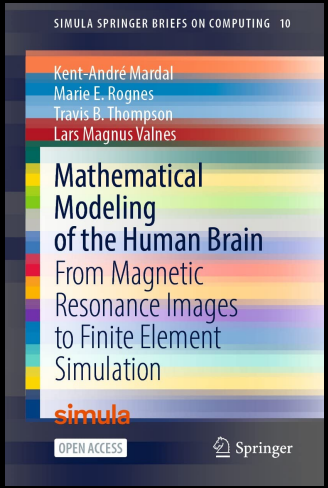

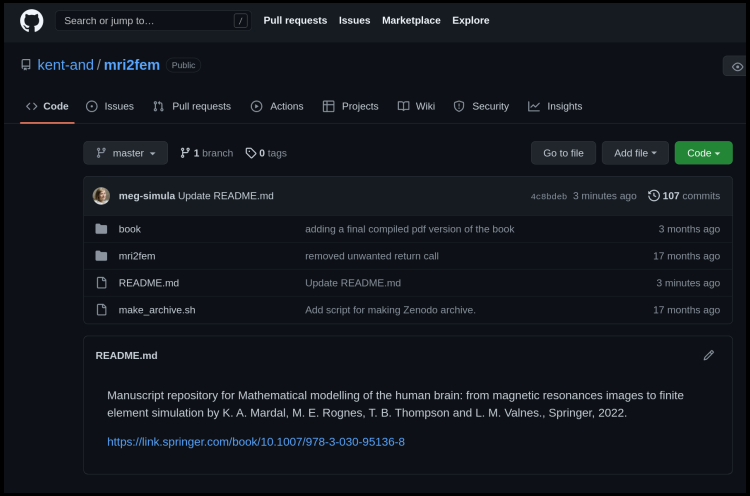

[https://github.com/kent-and/mri2fem]

Mathematical modeling of the human brain II: ~~the brains strike back~~ from glymphatics to deep learning

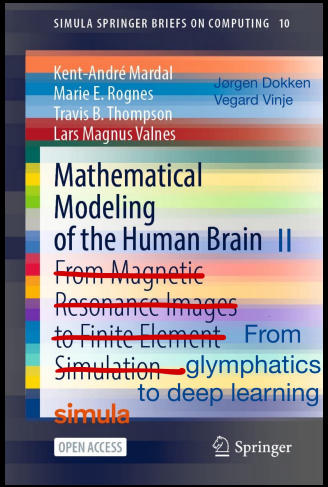

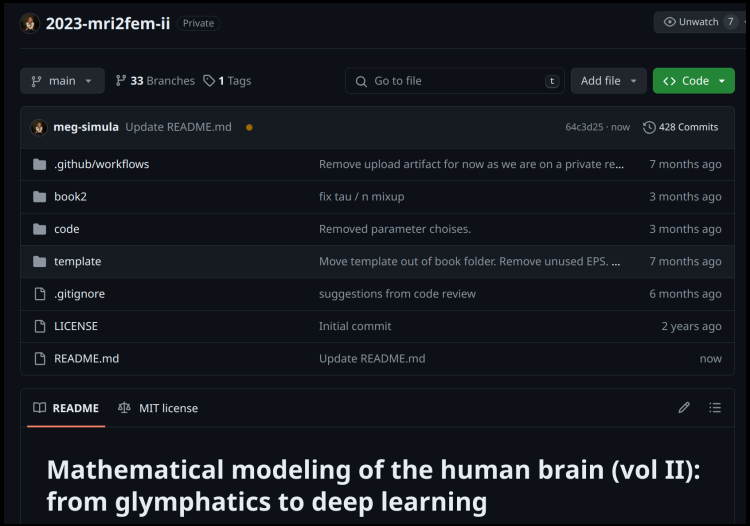

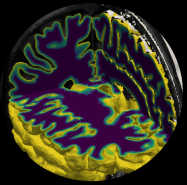

Solute transport and clearance

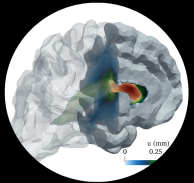

Brain mechanics

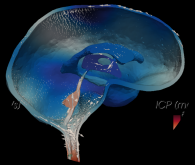

Cerebrospinal fluid flow and pulsatility

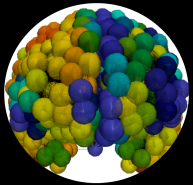

Neurodegeneration

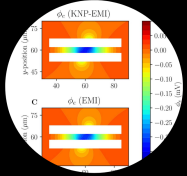

Ions and osmosis

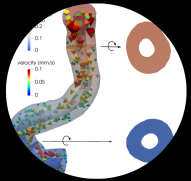

Mixed-dimensional PDEs

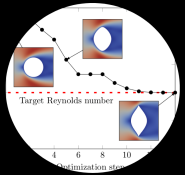

Optimization

Simulation technology

waterscales

simula

Acknowledgments and thanks

Pietro Benedusi
Nanna Berre
Marius Causemann
Cécile Daversin-Catty
Ada J. Ellingsrud
Ingeborg G. Gjerde
Halvor Herlyng
Martin Hornkjøl
Karoline Jæger
Miroslav Kuchta
Kent-Andre Mardal
Rami Masri
Marte-Julie Sætra
Lars-Magnus Valnes
Vegard Vinje
Bastian Zapf

Moritz Armbruster, Tufts U
Corrado Calí, U Torino
Matteo Croci, UT Austin/BCAM
Chris Dulla, Tufts U
Per-Kristian Eide, Oslo University Hospital
Rune Enger, U Oslo
Gaute Einevoll, Norwegian U of Life Scences
Geir Halnes, Norwegian U of Life Scences
Patrick E. Farrell, University of Oxford
Paola Ferrari, U Genova/Wuppertal
Emmet Francis, U California San Diego
Andre Massing, NTNU
Padmini Rangamani, U California San Diego
Chris N. Richardson, University of Cambridge
Geir Ringstad, Oslo University Hospital
Stefano Serra-Capizzano, U Insubria
Andreas Solbrå, U Oslo
Aslak Tveito, Simula
Marius Zeinhofer, Simua
Barbara Wohlmuth, TU Münich
... and many more ...

Cover illustration courtesy of Prof. Antonio Aráujo for the European Mathematical Society Magazine. This research is supported by the European Research Council (ERC) under the European Union's Horizon 2020 research and innovation programme under grant agreement 714892 (Waterscales), by the Research Council of Norway under grants #250731 (Waterscape) and #324239 (EMIx), by the EPSRC Centre For Doctoral Training in Industrially Focused 706 Mathematical Modelling (EP/L015803/1), by the Foundation Kristian Gerhard Jebsen via the K. G. Jebsen Center for Brain Fluid Research, and by the Wellcome Trust [#XXX].

Bibliography I

M. Abdellah, J. J. G. Cantero, N. R. Guerrero, A. Foni, J. S. Coggan, C. Calì, M. Agus, E. Zisis, D. Keller, M. Hadwiger, P. J. Magistretti, H. Markram, and F. Schürmann. Ultraliser: a framework for creating multiscale, high-fidelity and geometrically realistic 3D models for in silico neuroscience, Sept. 2022. URL `https://doi.org/10.5281/zenodo.7105941`.

A. Agudelo-Toro and A. Neef. Computationally efficient simulation of electrical activity at cell membranes interacting with self-generated and externally imposed electric fields. *Journal of neural engineering*, 10(2):026019, 2013.

M. Arioli and M. Benzi. A finite element method for quantum graphs. *IMA Journal of Numerical Analysis*, 38(3):1119–1163, 2018.

M. Asgari, D. De Zélicourt, and V. Kurtcuoglu. Glymphatic solute transport does not require bulk flow. *Scientific reports*, 6(1):38635, 2016.

F. Ben Belgacem, C. Bernardi, F. Jelassi, and M. Mint Brahim. Finite element methods for the temperature in composite media with contact resistance. *Journal of Scientific Computing*, 63:478–501, 2015.

P. Benedusi, P. Ferrari, M. E. Rognes, and S. Serra-Capizzano. Modeling excitable cells with the EMI equations: spectral analysis and iterative solution strategy. *Journal of Scientific Computing*, 98(3):58, 2024.

G. Berkolaiko and P. Kuchment. *Introduction to quantum graphs*. Number 186. American Mathematical Soc., 2013.

W. M. Boon, J. M. Nordbotten, and J. E. Vatne. Functional analysis and exterior calculus on mixed-dimensional geometries. *Annali di Matematica Pura ed Applicata (1923-)*, 200(2): 757–789, 2021.

C. Calì, M. Agus, K. Kare, D. J. Boges, H. Lehväslaiho, M. Hadwiger, and P. J. Magistretti. 3D cellular reconstruction of cortical glia and parenchymal morphometric analysis from serial block-face electron microscopy of juvenile rat. *Progress in neurobiology*, 183:101696, 2019.

M. Causemann, V. Vinje, and M. E. Rognes. Human intracranial pulsatility during the cardiac cycle: a computational modelling framework. *Fluids and Barriers of the CNS*, 19(1):84, 2022.

C. Daversin-Catty, V. Vinje, K.-A. Mardal, and M. E. Rognes. The mechanisms behind perivascular fluid flow. *Plos one*, 15(12):e0244442, 2020.

C. Daversin-Catty, I. G. Gjerde, and M. E. Rognes. Geometrically reduced modelling of pulsatile flow in perivascular networks. *Frontiers in Physics*, 10:882260, 2022.

L. B. Flexner. Some problems of the origin, circulation and absorption of the cerebrospinal fluid. *The Quarterly Review of Biology*, 8(4):397–422, 1933.

L. Formaggia, D. Lamponi, and A. Quarteroni. One-dimensional models for blood flow in arteries. *Journal of engineering mathematics*, 47:251–276, 2003.

I. Gjerde, M. Rognes, and A. Sánchez. The directional flow generated by peristalsis in perivascular networks-theoretical and numerical reduced-order descriptions. *Journal of Applied Physics*, 134(17):174701–174701, 2023.

I. G. Gjerde, M. Kuchta, M. E. Rognes, and B. Wohlmuth. Directional flow in perivascular networks: Mixed finite elements for reduced-dimensional models on graphs. *arXiv preprint arXiv:2401.00484*, 202X.

Bibliography II

P. Hadaczek, Y. Yamashita, H. Mirek, L. Tamas, M. C. Bohn, C. Noble, J. W. Park, and K. Bankiewicz. The “perivascular pump” driven by arterial pulsation is a powerful mechanism for the distribution of therapeutic molecules within the brain. *Molecular Therapy*, 14(1):69–78, 2006.

W. His. *Über ein perivasculäres Canalsytem in den nervösen Centralorganen und über dessen Beziehungen zum Lymphsystem: Mit einer in Farben gedruckten Tafel.* W. Engelmann, 1865.

E. Hodneland, E. Hanson, O. Sævareid, G. Nævdal, A. Lundervold, V. Šoltészová, A. Z. Munthe-Kaas, A. Deistung, J. R. Reichenbach, and J. M. Nordbotten. A new framework for assessing subject-specific whole brain circulation and perfusion using mri-based measurements and a multi-scale continuous flow model. *PLoS computational biology*, 15(6): e1007073, 2019.

M. Hornkjøl, L. M. Valnes, G. Ringstad, M. E. Rognes, P.-K. Eide, K.-A. Mardal, and V. Vinje. CSF circulation and dispersion yield rapid clearance from intracranial compartments. *Frontiers in Bioengineering and Biotechnology*, 10:932469, 2022.

T. Ichimura, P. Fraser, and H. F. Cserr. Distribution of extracellular tracers in perivascular spaces of the rat brain. *Brain research*, 545(1-2):103–113, 1991.

J. J. Iliff, M. Wang, Y. Liao, B. A. Plogg, W. Peng, G. A. Gundersen, H. Benveniste, G. E. Vates, R. Deane, S. A. Goldman, et al. A paravascular pathway facilitates csf flow through the brain parenchyma and the clearance of interstitial solutes, including amyloid β. *Science translational medicine*, 4(147):147ra111–147ra111, 2012.

M. Kuchta, K.-A. Mardal, and M. E. Rognes. Solving the EMI equations using finite element methods. *Modeling Excitable Tissue: The EMI Framework*, pages 56–69, 2021.

J. G. Laughlin, J. S. Dokken, H. N. Finsberg, E. A. Francis, C. T. Lee, M. E. Rognes, and P. Rangamani. SMART: spatial modeling algorithms for reactions and transport. *The Journal of Open Source Software*, 8(90):5580, 2023.

A. D. Martinac and L. E. Bilston. Computational modelling of fluid and solute transport in the brain. *Biomechanics and modeling in mechanobiology*, 19:781–800, 2020.

R. Masri, M. Zeinhofer, M. Kuchta, and M. E. Rognes. The modelling error in multi-dimensional time-dependent solute transport models. *ESAIM: M2AN*, 2024.

R. Masri, M. Causemann, M. Kuchta, and M. E. Rognes. In-silico molecular transport in the human brain. *In preparation*, 202X.

H. Mestre, J. Tithof, T. Du, W. Song, W. Peng, A. M. Sweeney, G. Olveda, J. H. Thomas, M. Nedergaard, and D. H. Kelley. Flow of cerebrospinal fluid is driven by arterial pulsations and is reduced in hypertension. *Nature communications*, 9(1):4878, 2018.

A. Motta, M. Berning, K. M. Boergens, B. Staffler, M. Beining, S. Loomba, P. Hennig, H. Wissler, and M. Helmstaedter. Dense connectomic reconstruction in layer 4 of the somatosensory cortex. *Science*, 366(6469):eaay3134, 2019.

M. S. Olufsen. Structured tree outflow condition for blood flow in larger systemic arteries. *American journal of physiology-Heart and circulatory physiology*, 276(1):H257–H268, 1999.

M. L. Rennels, T. F. Gregory, O. R. Blaumanis, K. Fujimoto, and P. A. Grady. Evidence for a "paravascular" fluid circulation in the mammalian central nervous system, provided by the rapid distribution of tracer protein throughout the brain from the subarachnoid space. *Brain research*, 326(1):47–63, 1985.

G. Ringstad, S. A. S. Vatnehol, and P. K. Eide. Glymphatic mri in idiopathic normal pressure hydrocephalus. *Brain*, 140(10):2691–2705, 2017.

Bibliography III

G. Ringstad, L. M. Valnes, A. M. Dale, A. H. Pripp, S.-A. S. Vatnehol, K. E. Emblem, K.-A. Mardal, and P. K. Eide. Brain-wide glymphatic enhancement and clearance in humans assessed with mri. *JCI insight*, 3(13), 2018.

J. San Martín, L. Smaranda, and T. Takahashi. Convergence of a finite element/ale method for the stokes equations in a domain depending on time. *Journal of computational and applied mathematics*, 230(2):521–545, 2009.

L. M. Sangalli, P. Secchi, and S. Vantini. Aneurisk65: A dataset of three-dimensional cerebral vascular geometries. 2014.

J. Stinstra, R. MacLeod, and C. Henriquez. Incorporating histology into a 3d microscopic computer model of myocardium to study propagation at a cellular level. *Annals of biomedical engineering*, 38:1399–1414, 2010.

J. H. Thomas. Fluid dynamics of cerebrospinal fluid flow in perivascular spaces. *Journal of the Royal Society Interface*, 16(159):20190572, 2019.

A. Tveito, K. H. Jæger, M. Kuchta, K.-A. Mardal, and M. E. Rognes. A cell-based framework for numerical modeling of electrical conduction in cardiac tissue. *Frontiers in Physics*, 5: 48, 2017.

A. Tveito, K.-A. Mardal, and M. E. Rognes. *Modeling excitable tissue: The EMI framework*. Springer Nature, 2021.

B. I. Wohlmuth. A mortar finite element method using dual spaces for the lagrange multiplier. *SIAM journal on numerical analysis*, 38(3):989–1012, 2000.